

Constraining the EOS from flow and the QCD CP from proton fluctuations

Agnieszka Sorensen

Facility for Rare Isotope Beams

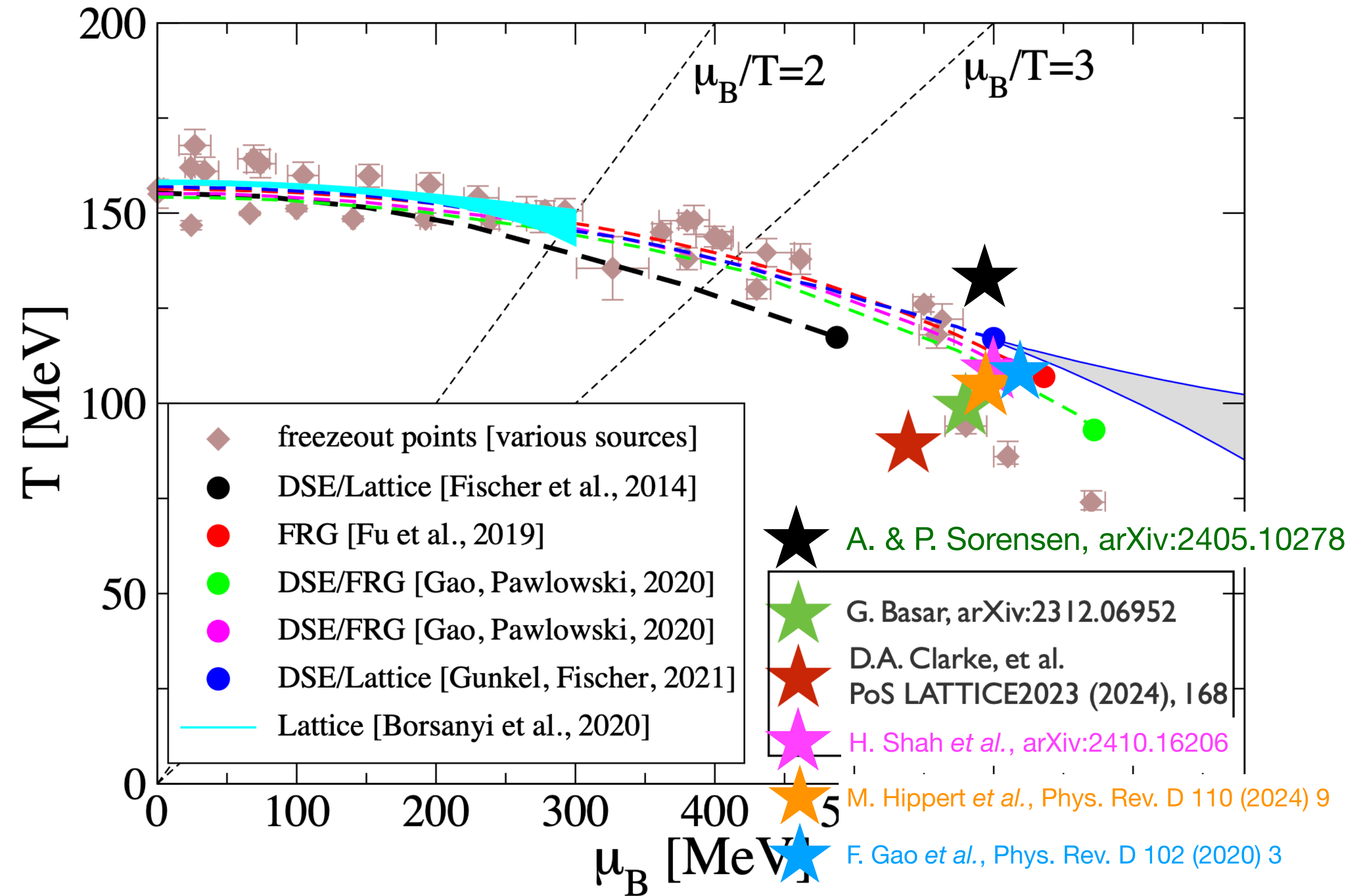
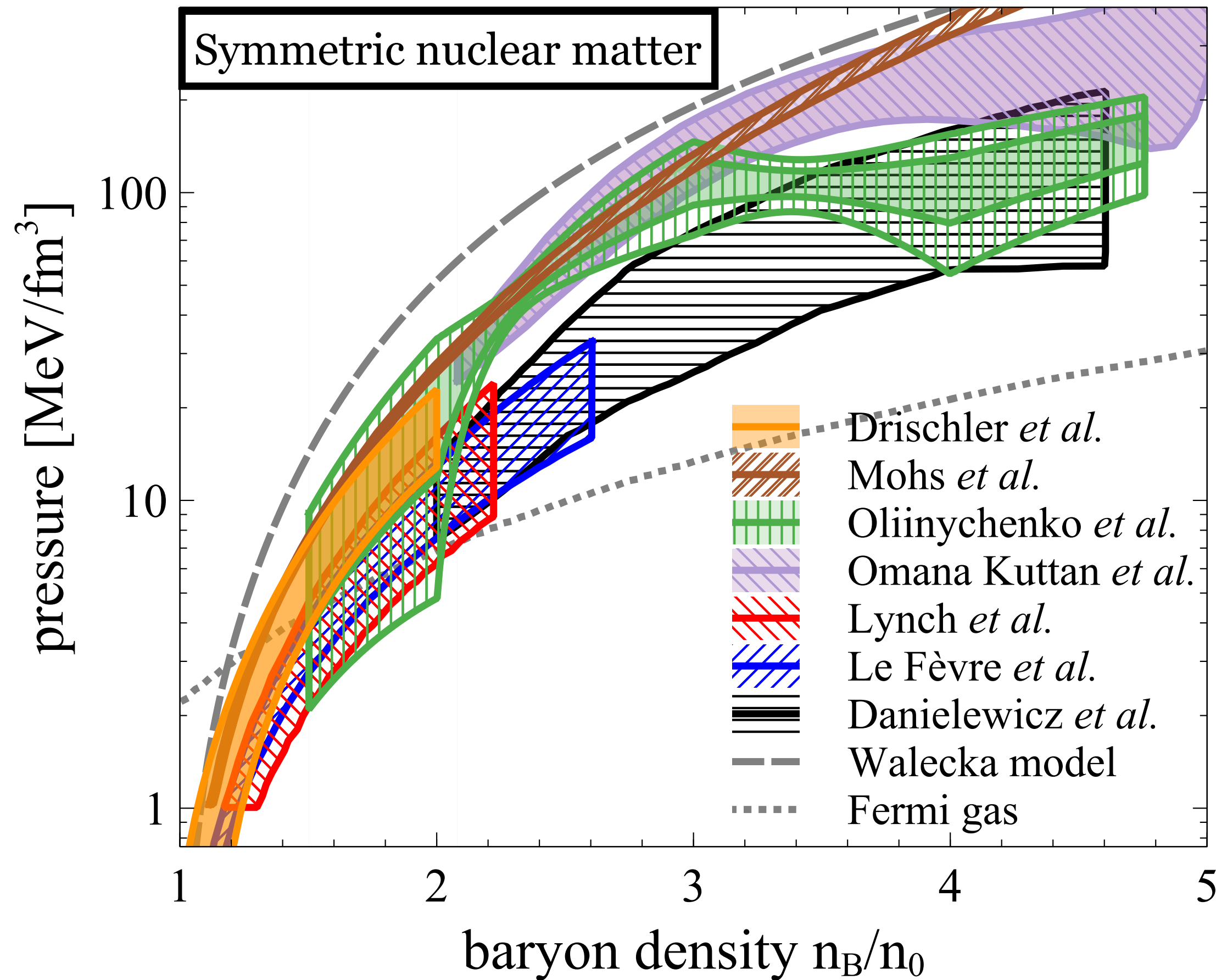
Michigan State University

Phys. Rev. C 108 (2023) 3, 034908 ([arXiv:2208.11996](https://arxiv.org/abs/2208.11996))
[arXiv:2405.10278](https://arxiv.org/abs/2405.10278)



Selected recent results

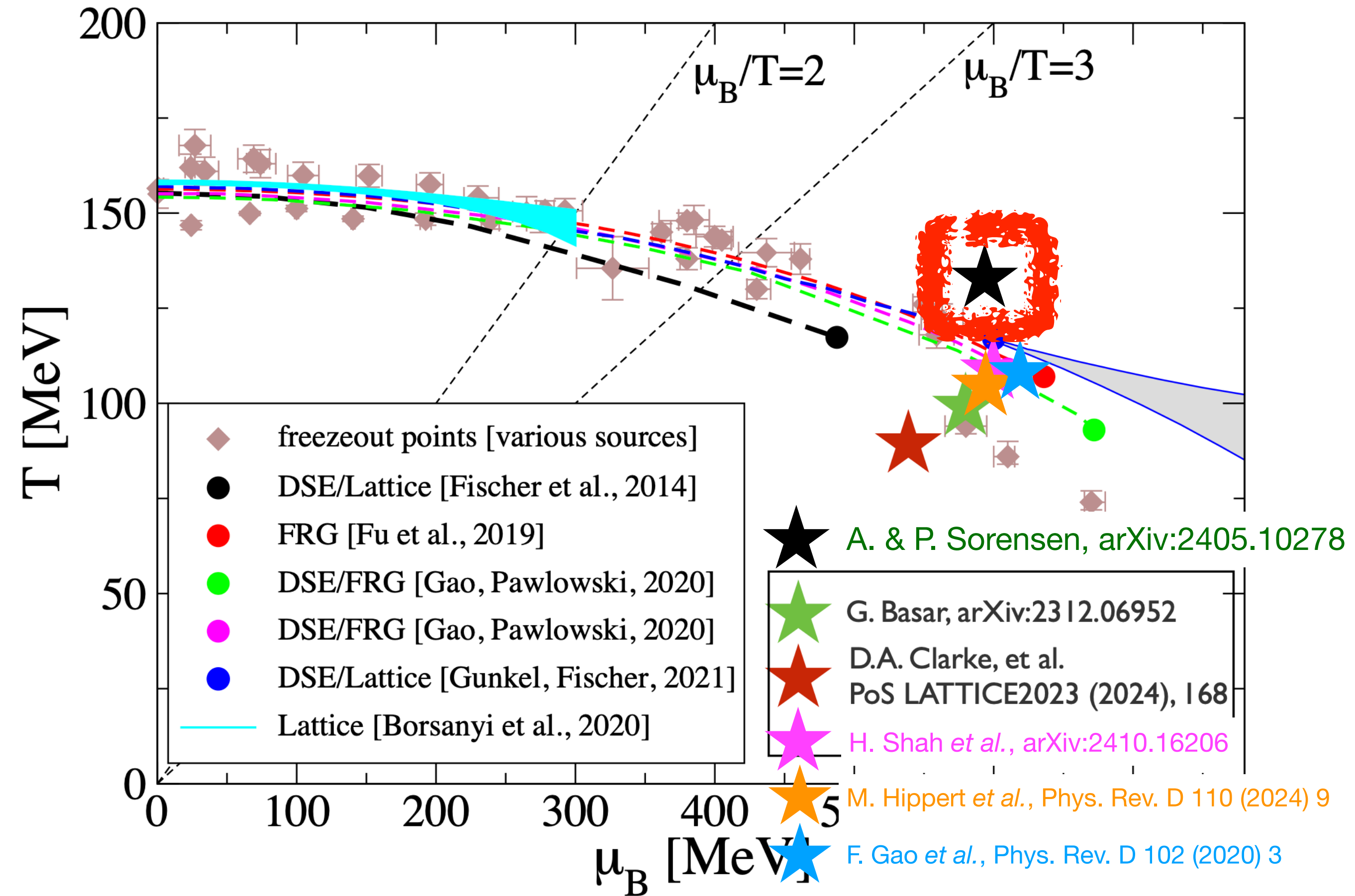
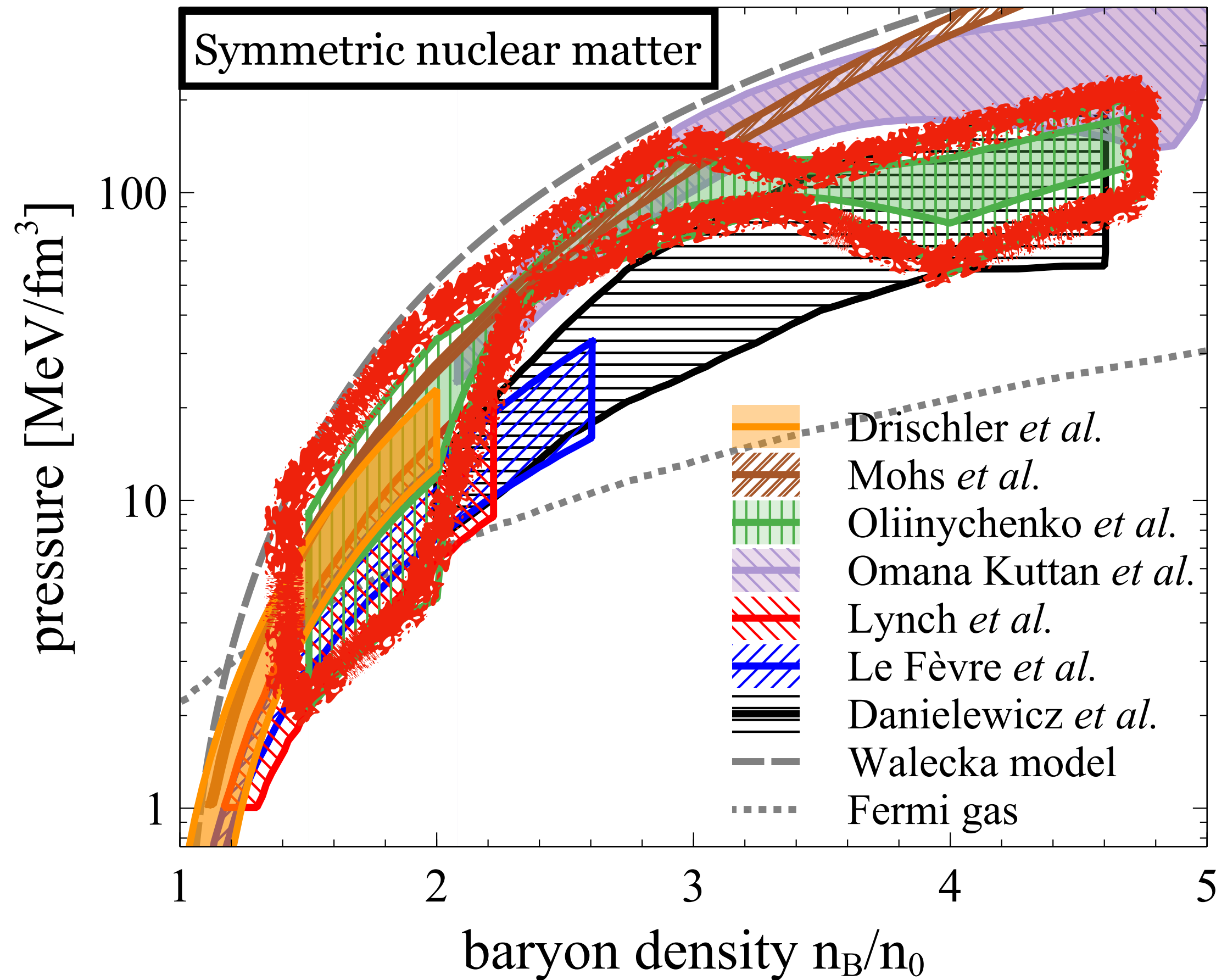
- constraints on the n_B -dependence of the EOS: χ EFT, transport model comparisons: old (3) and new (3)
- constraints on the QCD critical point: LQCD-based (3), holography+LQCD (1), FRG(1), STAR data (1)



adapted from Christian Fischer, CPOD 2024

Selected recent results

- constraints on the n_B -dependence of the EOS: χ EFT, transport model comparisons: old (3) and new (3)
- constraints on the QCD critical point: LQCD-based (3), holography+LQCD (1), FRG(1), STAR data (1)
- I'm going to mainly discuss my work

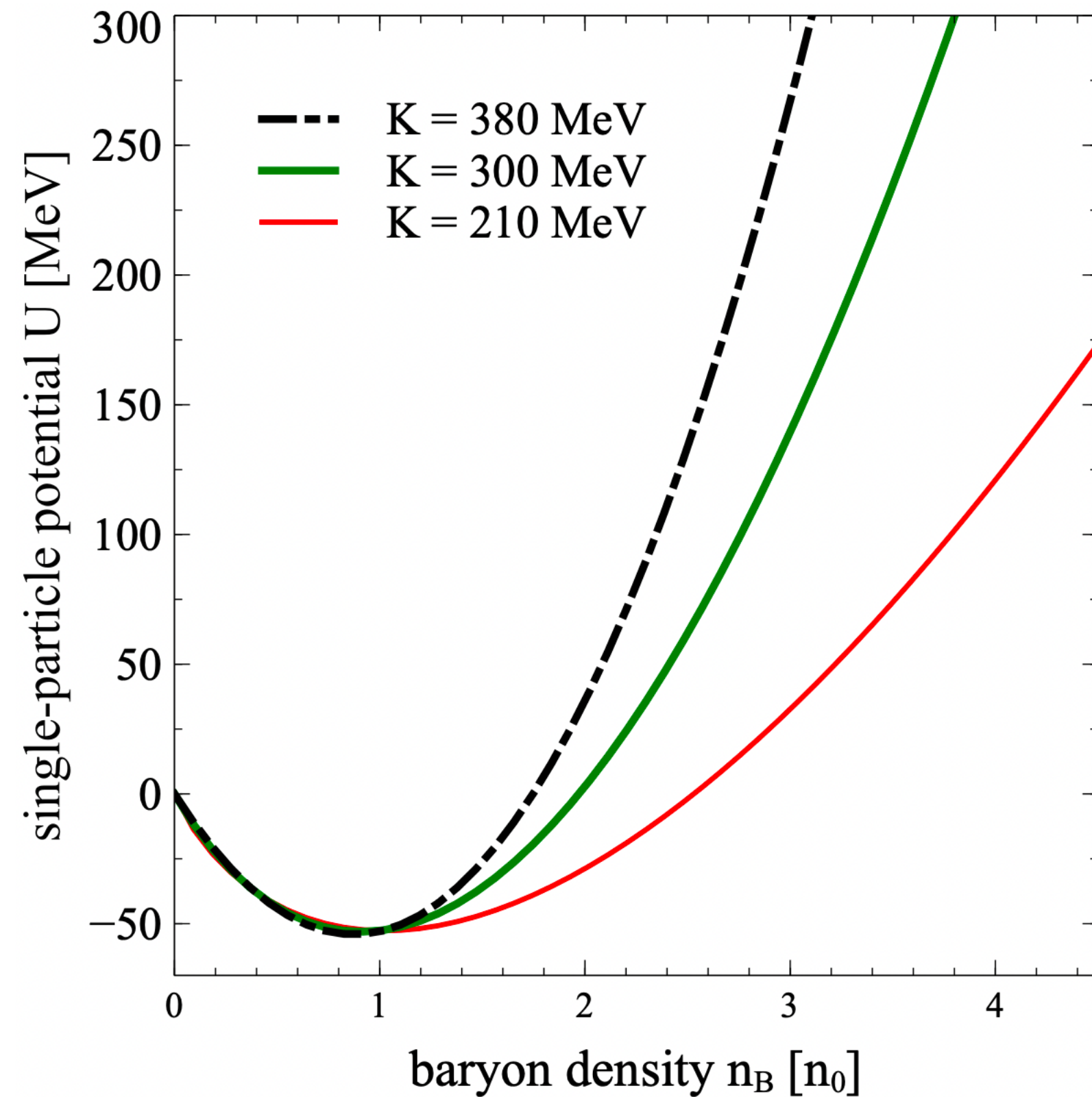


adapted from Christian Fischer, CPOD 2024

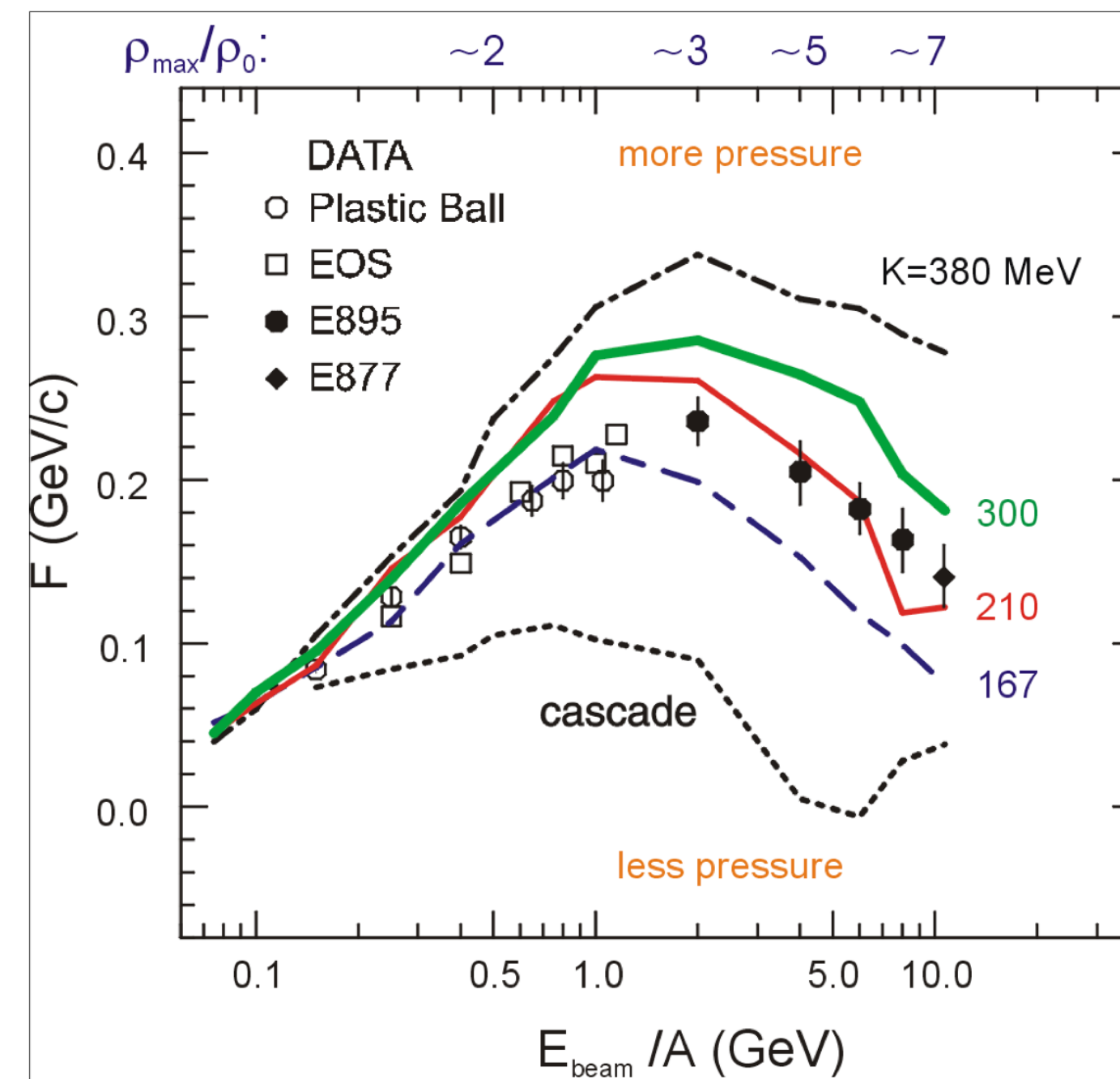
Flow results

Standard way of modeling the EOS: Skyrme potential

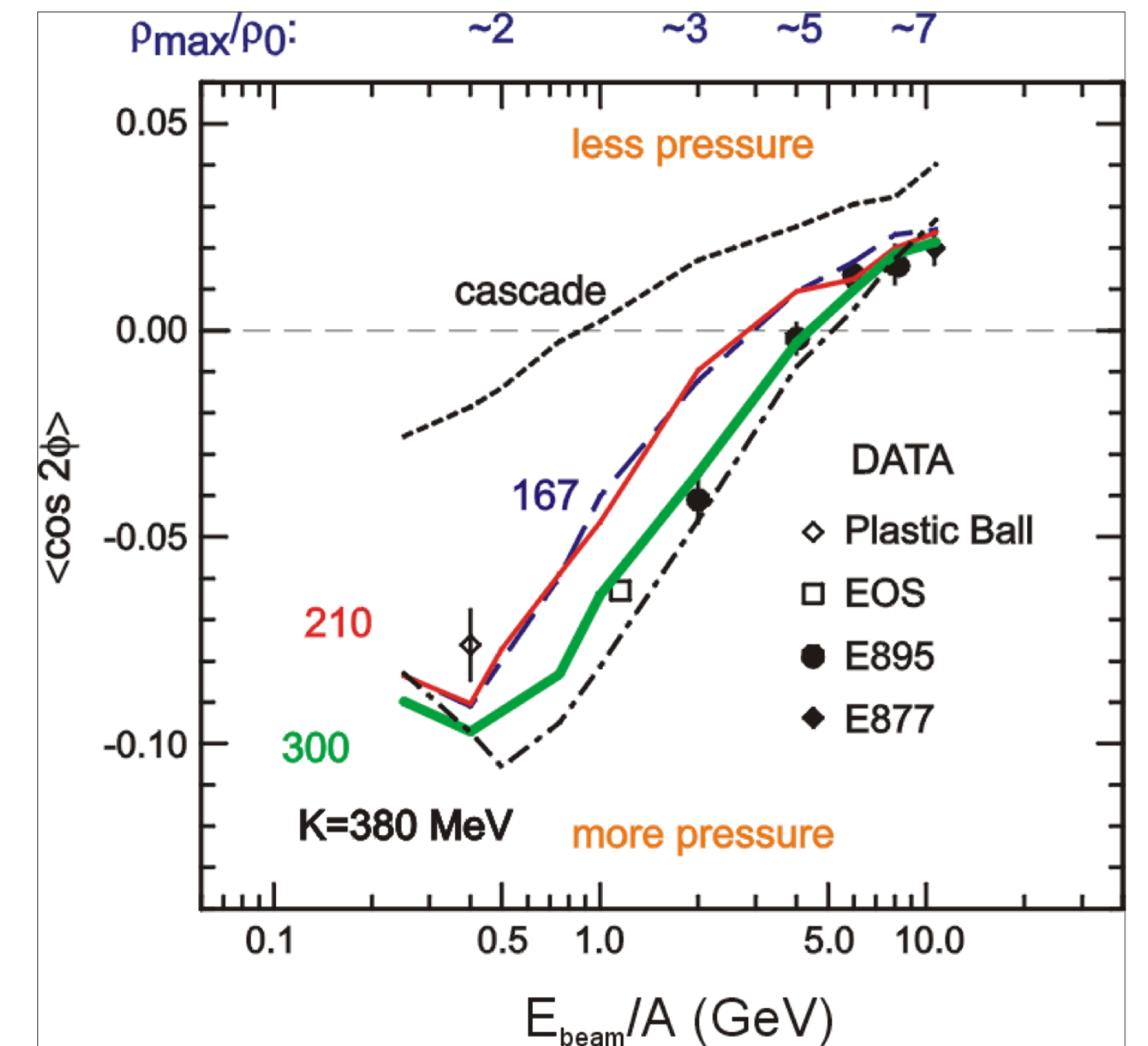
The most common form of the EOS is the “Skyrme potential”: $U(n_B) = A \left(\frac{n_B}{n_0} \right) + B \left(\frac{n_B}{n_0} \right)^\tau$



$$F = \left. \frac{d\langle p_x/A \rangle}{d(y/y_{cm})} \right|_{v/v_1 = 1} \sim \frac{dv_1}{dy}$$



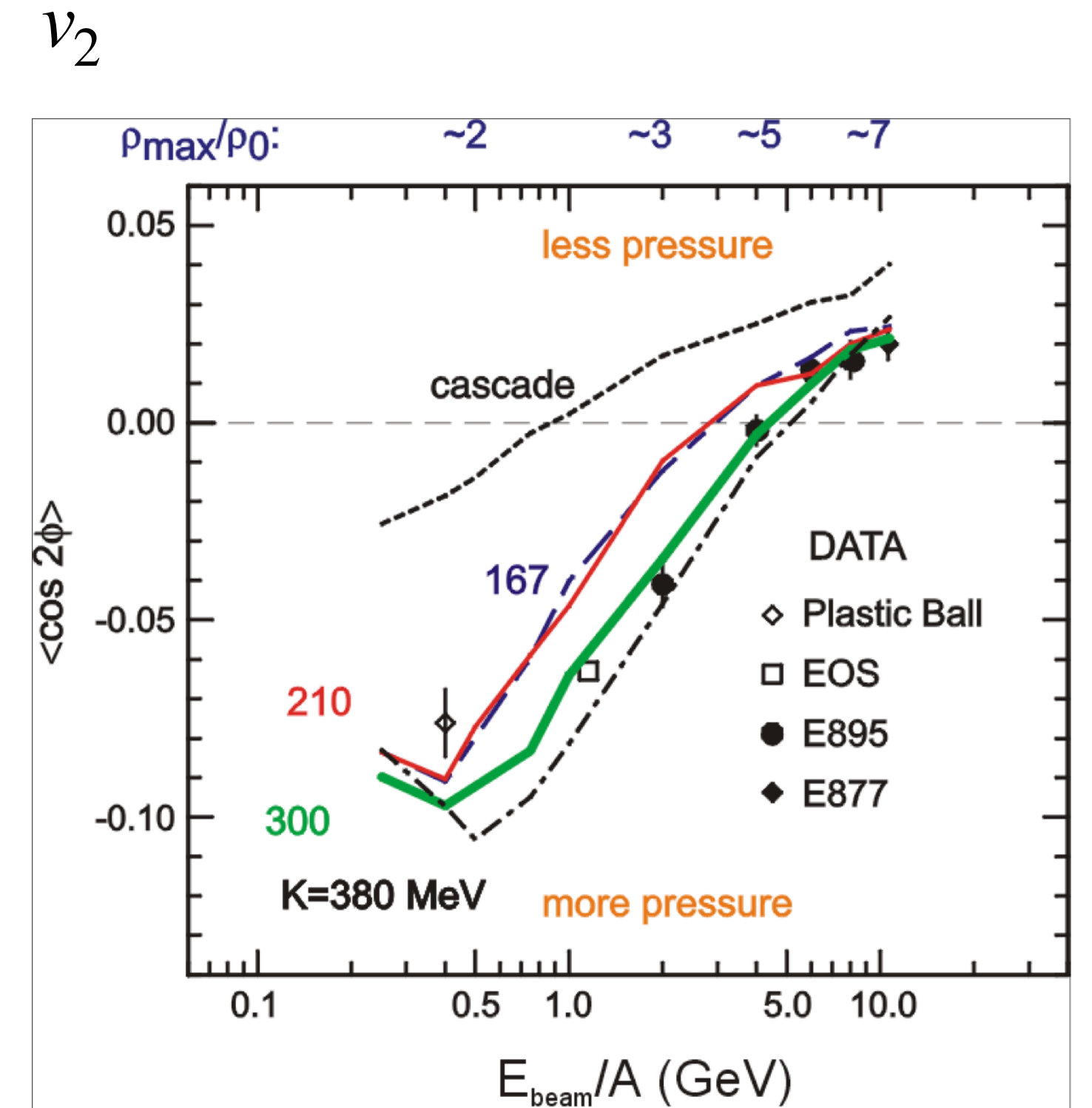
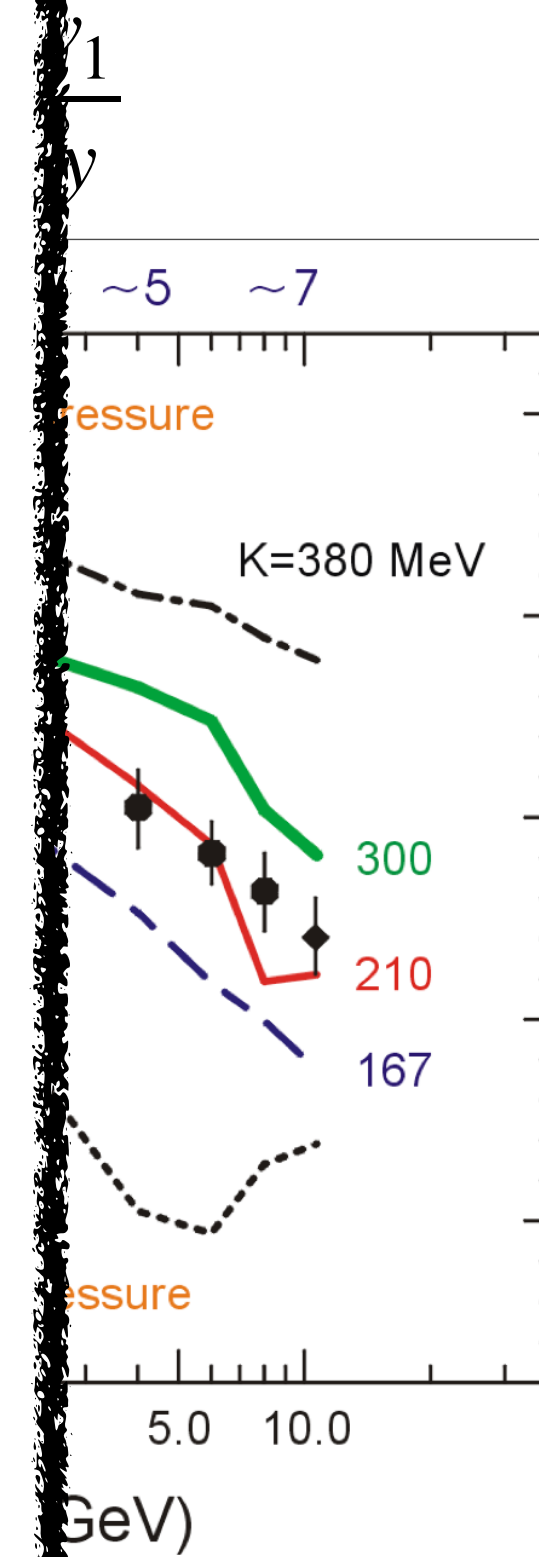
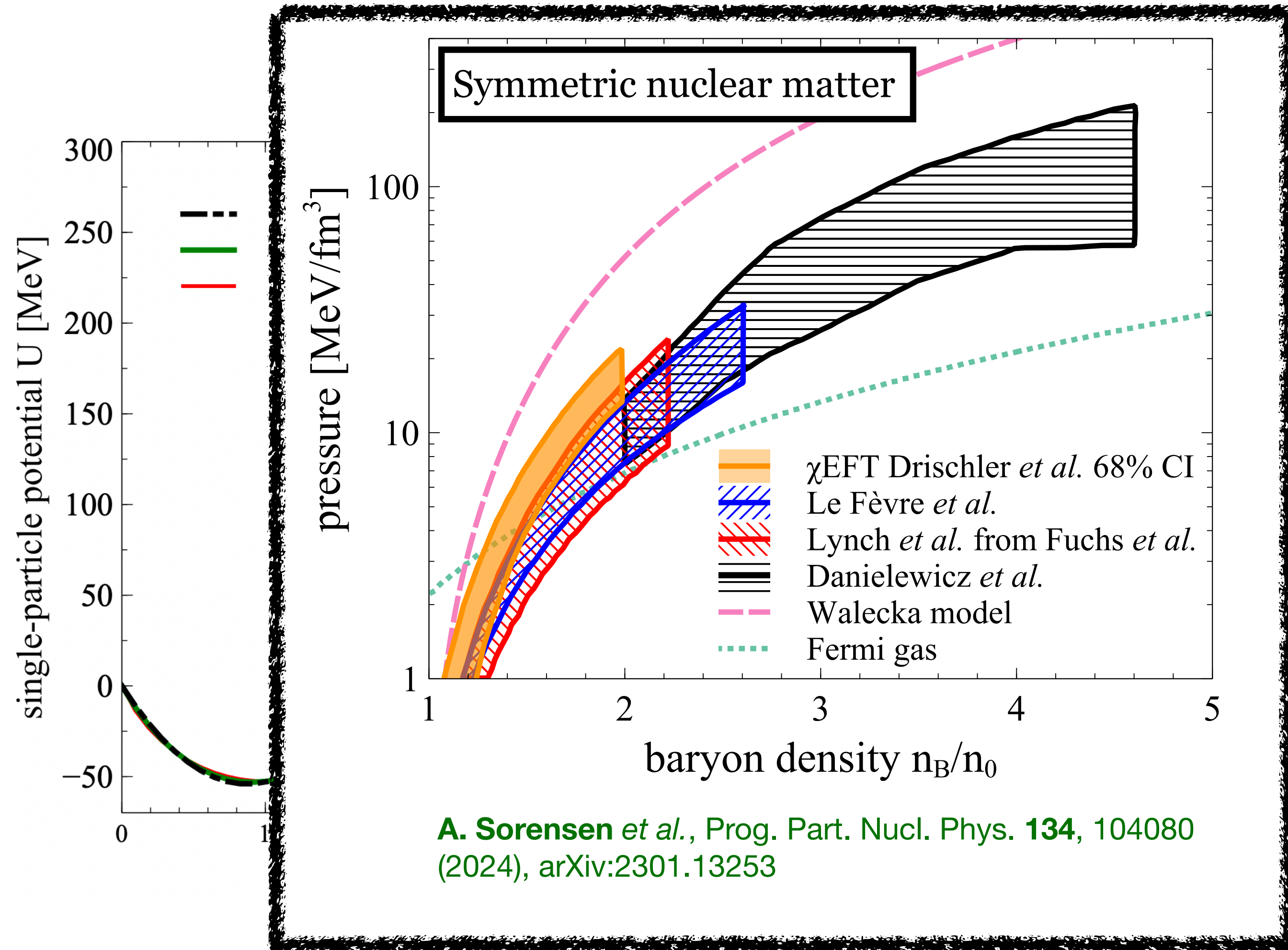
v_2



P. Danielewicz, R. Lacey, W. G. Lynch,
 Science **298**, 1592–1596 (2002), arXiv:nucl-th/0208016

Standard way of modeling the EOS: Skyrme potential

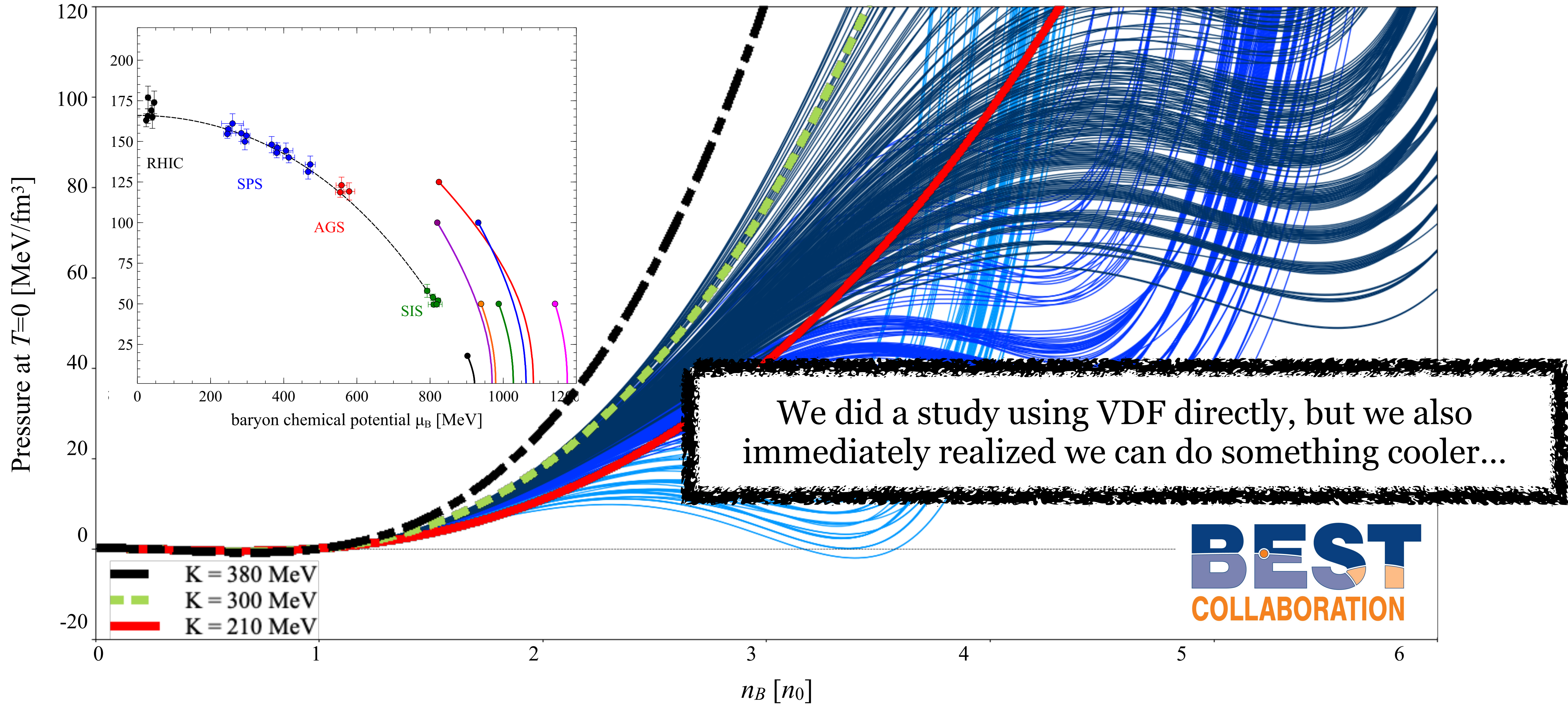
The most common form of the EOS is the “Skyrme potential”: $U(n_B) = A \left(\frac{n_B}{n_0} \right) + B \left(\frac{n_B}{n_0} \right)^\tau$



P. Danielewicz, R. Lacey, W. G. Lynch, Science **298**, 1592–1596 (2002), arXiv:nucl-th/0208016

VDF model: relativistic potentials with **two** 1st order phase transitions

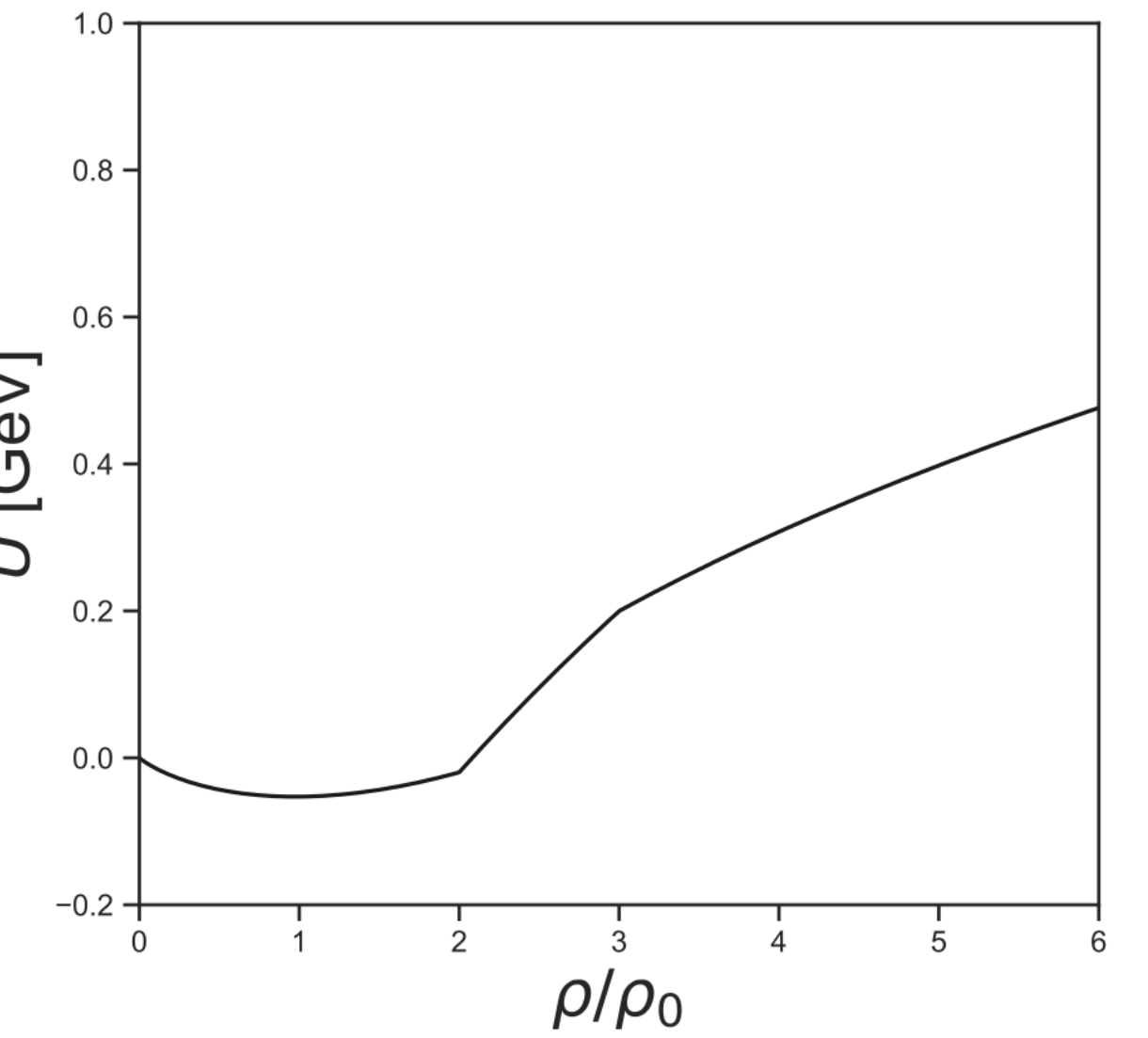
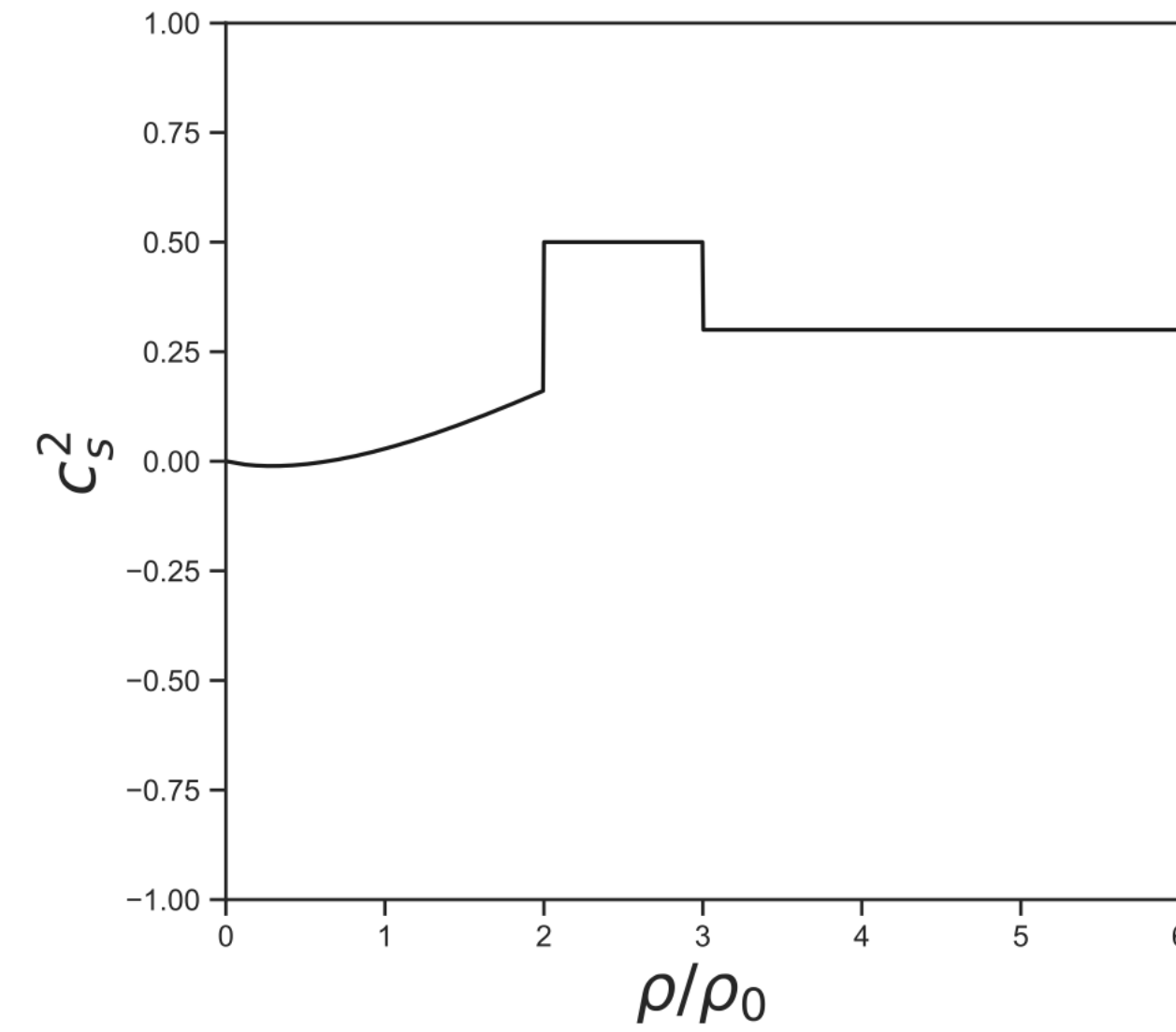
A. Sorensen, V. Koch, Phys. Rev. C **104** (2021) 3, 034904, arXiv:2011.06635



Piecewise parametrization of c_s^2

Piecewise parametrization of $c_s^2(n_B)$:

$$c_s^2(n_B) = \begin{cases} c_s^2(\text{Skyrme}), & n_B < n_1 = 2n_0 \\ c_1^2, & n_1 < n_B < n_2 \\ c_2^2, & n_2 < n_B < n_3 \\ \dots & \\ c_m^2, & n_m < n_B \end{cases}$$



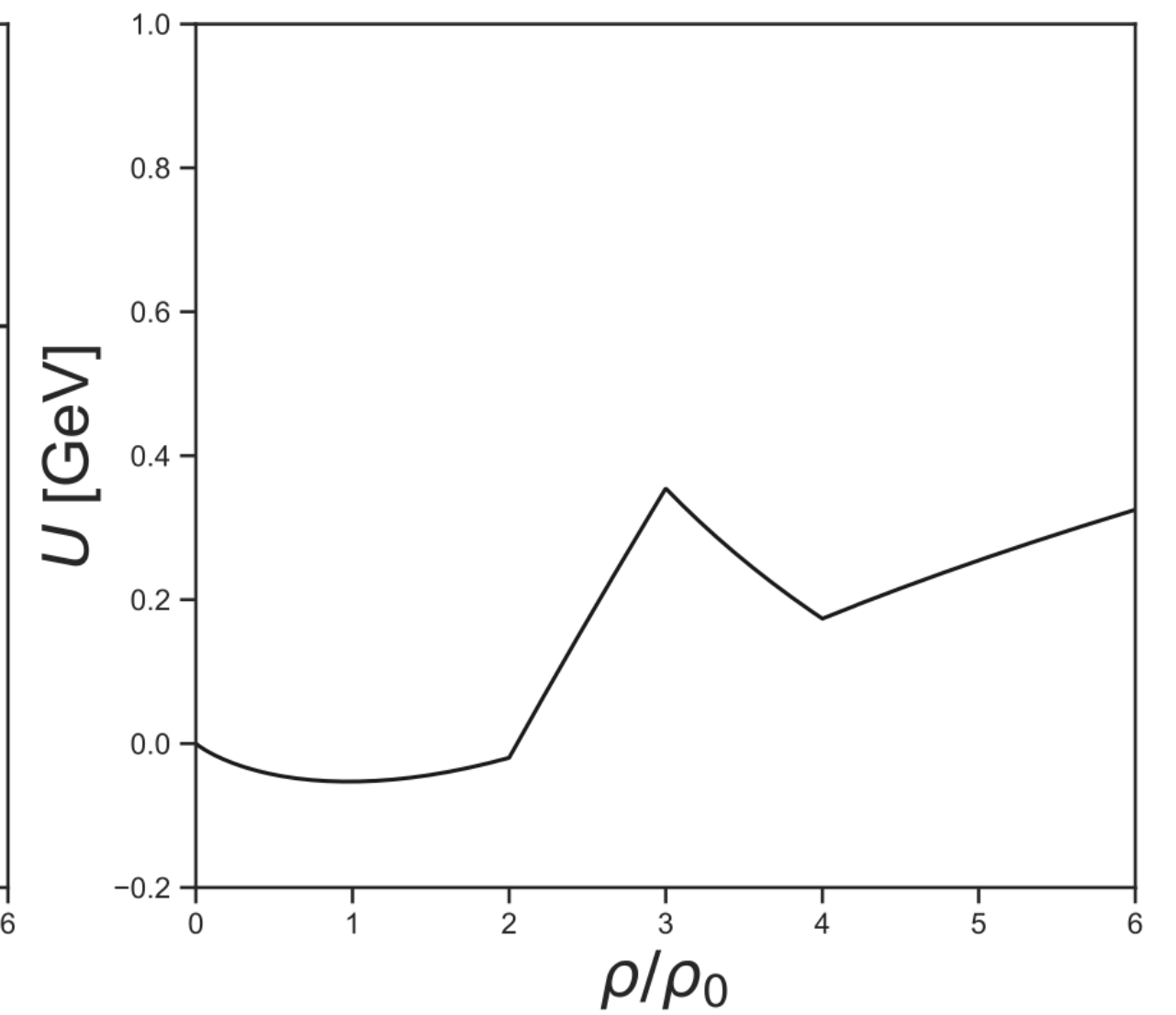
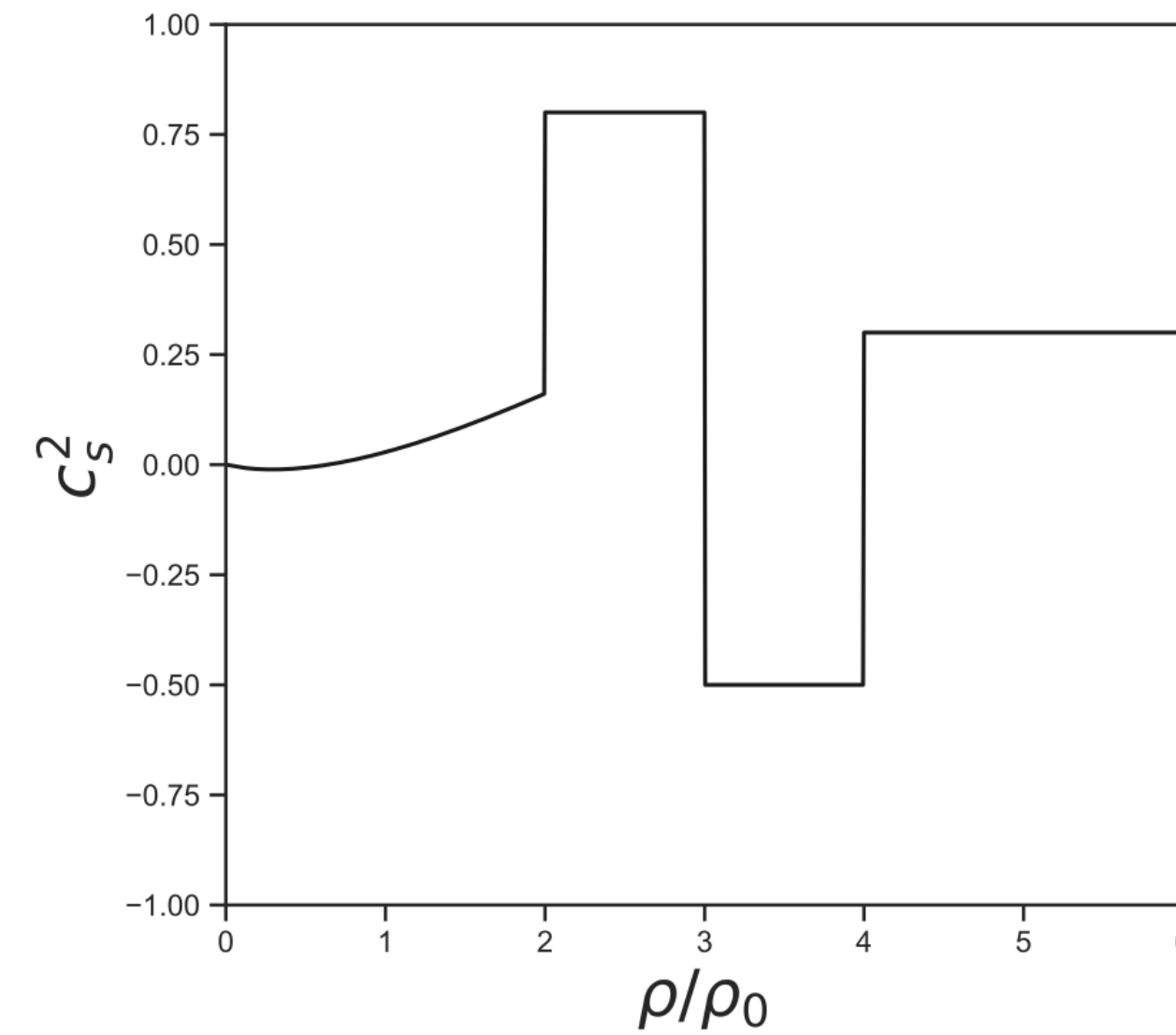
1-to-1 relation to the single-particle potential $U(n_B)$:

$$U(n_B) = \begin{cases} U_{\text{Sk}}(n_B) & n_B < n_1 = 2n_0 \\ U_1(n_B) & n_1 < n_B < n_2 \\ \dots & \\ U_k(n_B) & n_k < n_B < n_{k+1} \end{cases}$$

Piecewise parametrization of c_s^2

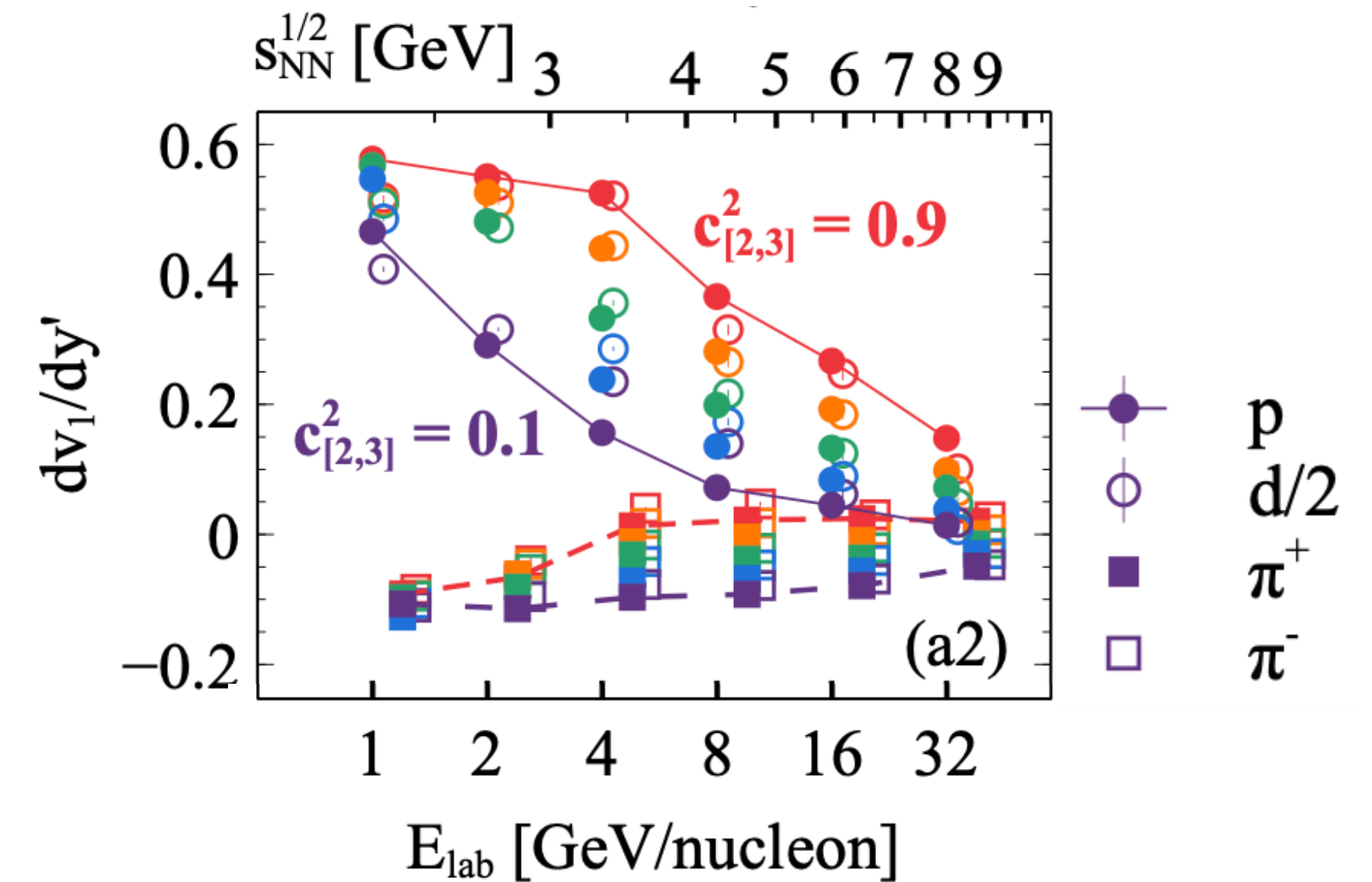
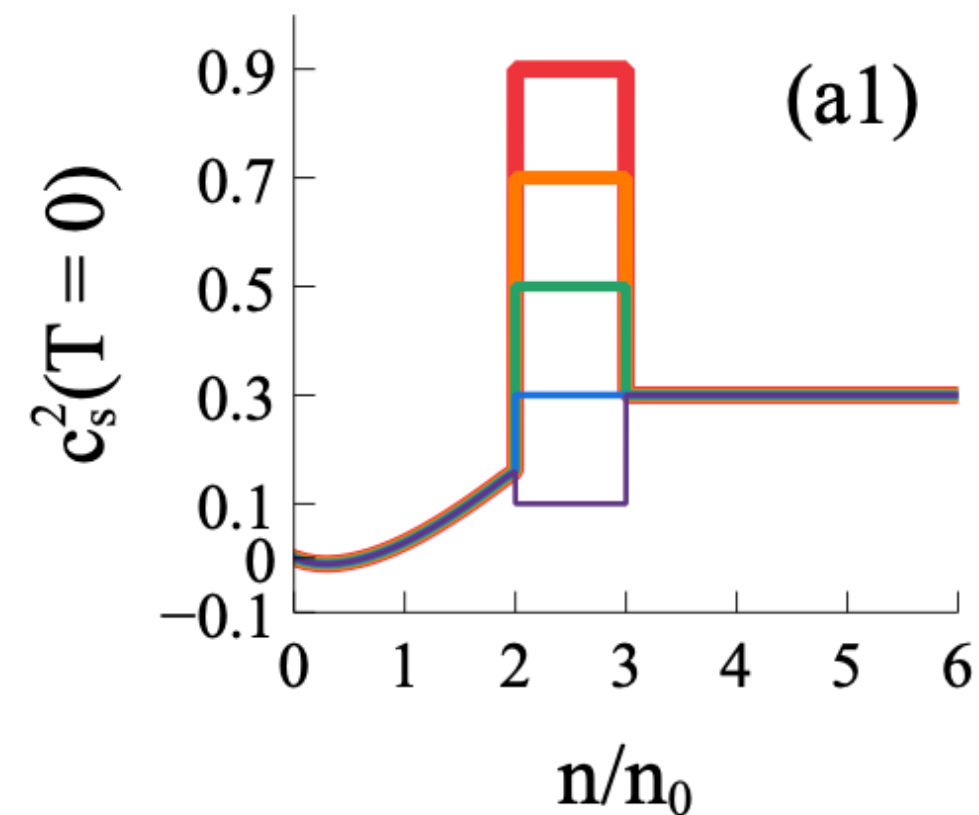
Piecewise parametrization of $c_s^2(n_B)$:

$$c_s^2(n_B) = \begin{cases} c_s^2(\text{Skyrme}), & n_B < n_1 = 2n_0 \\ c_1^2, & n_1 < n_B < n_2 \\ c_2^2, & n_2 < n_B < n_3 \\ \dots & \\ c_m^2, & n_m < n_B \end{cases}$$



1-to-1 relation to the single-particle potential $U(n_B)$:

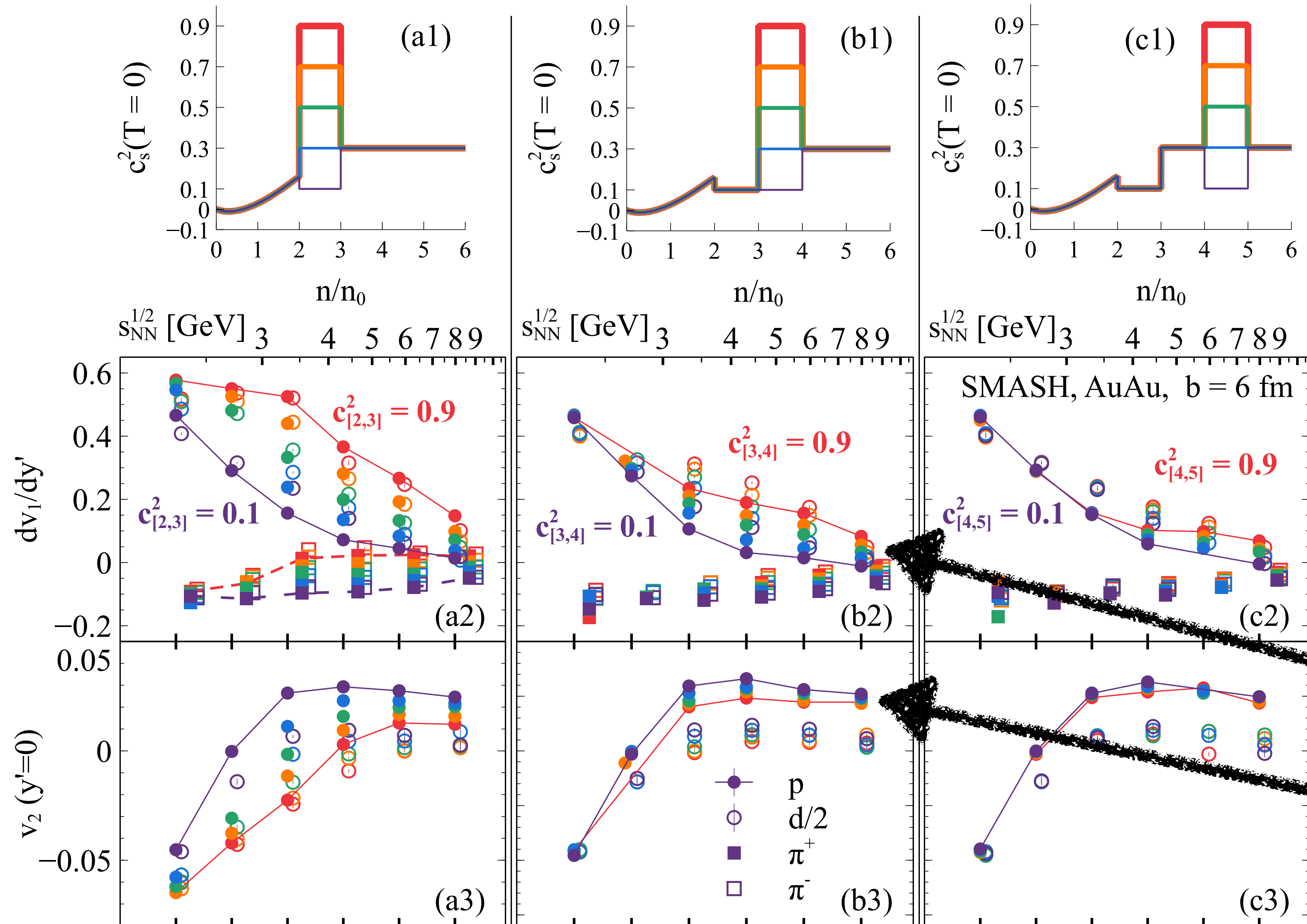
$$U(n_B) = \begin{cases} U_{\text{Sk}}(n_B) & n_B < n_1 = 2n_0 \\ U_1(n_B) & n_1 < n_B < n_2 \\ \dots & \\ U_k(n_B) & n_k < n_B < n_{k+1} \end{cases}$$



D. Oliinychenko, A. Sorensen, V. Koch, L. McLerran,
Phys. Rev. C **108**, 3, 034908 (2023), arXiv:2208.11996

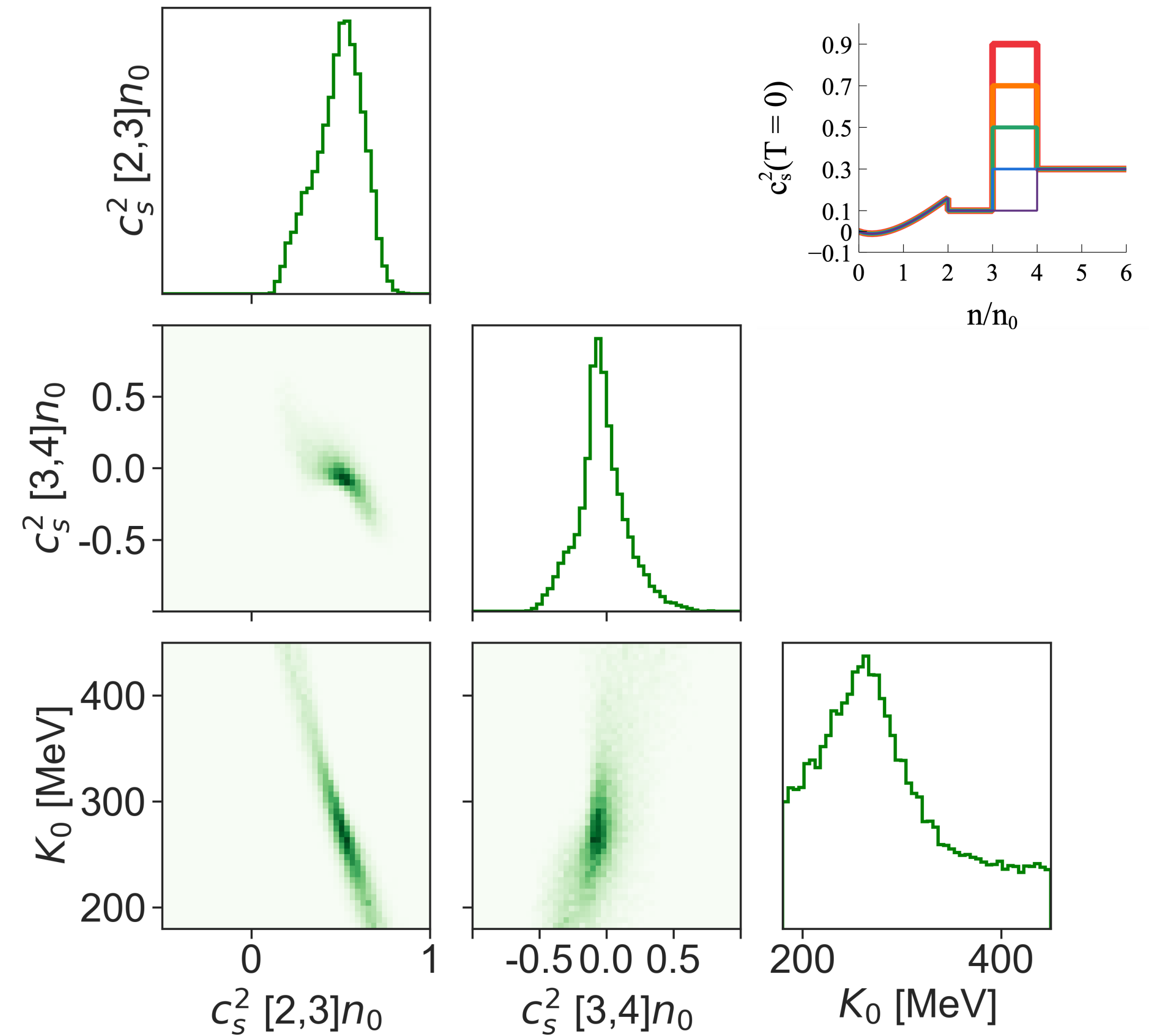
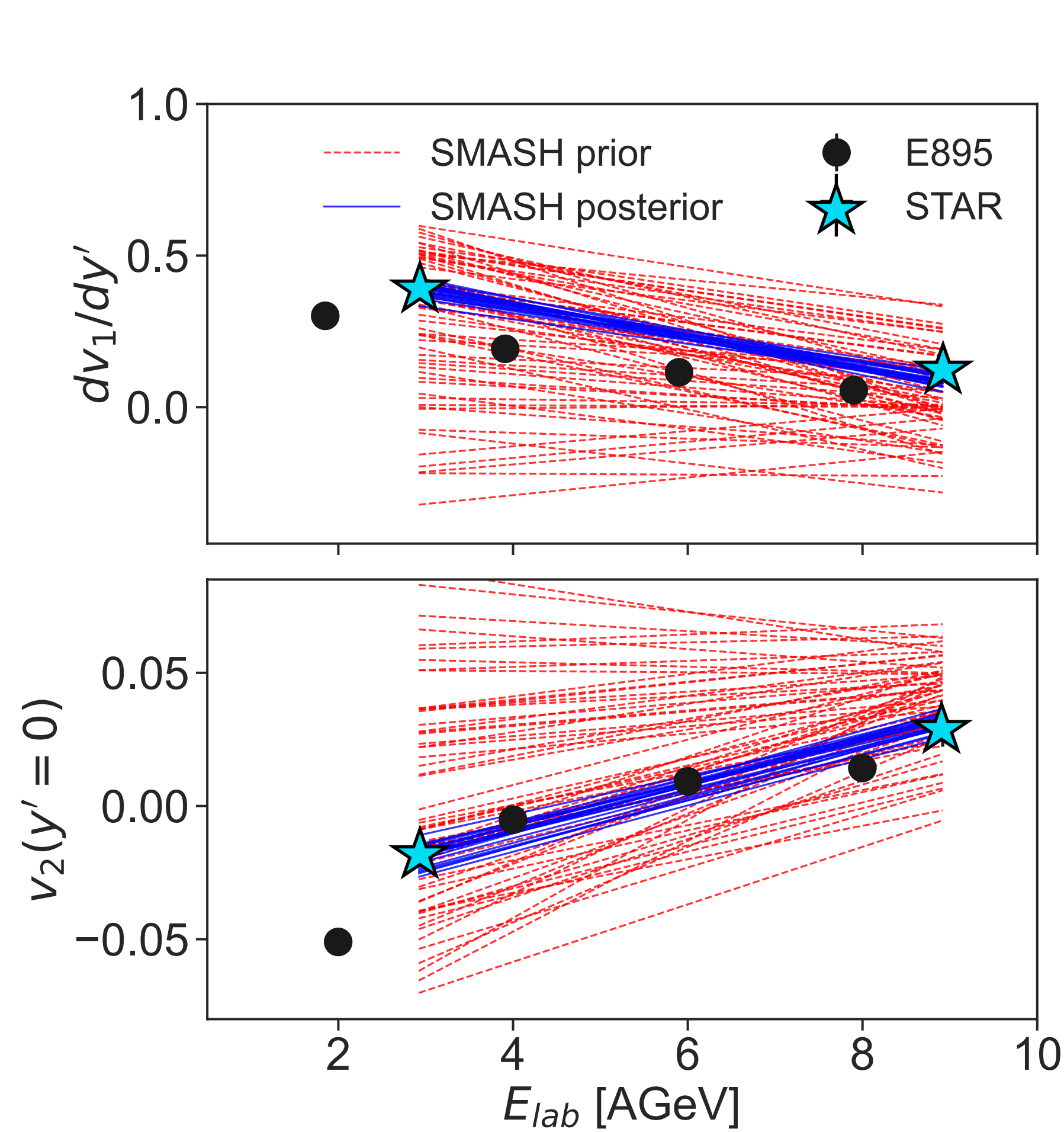
Sensitivity of proton flow to the EOS

D. Oliinychenko, A. Sorensen, V. Koch, L. McLerran,
 Phys. Rev. C **108**, 3, 034908 (2023), arXiv:2208.11996



proton v_1 is needed
 to constrain the EOS
 at high density

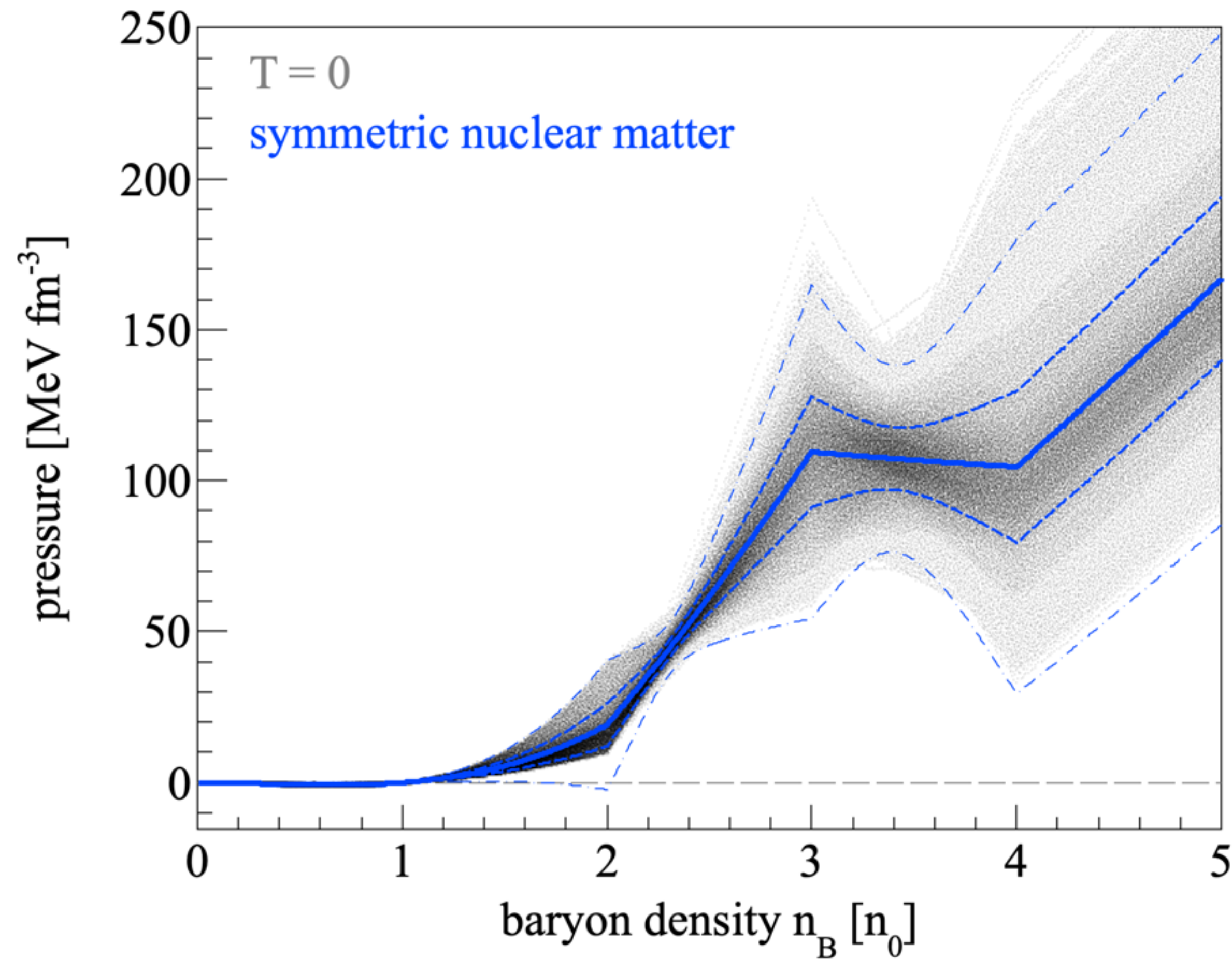
Bayesian analysis of BES flow in SMASH with varying K_0 , $c_{[2,3]n_0}^2$, $c_{[3,4]n_0}^2$



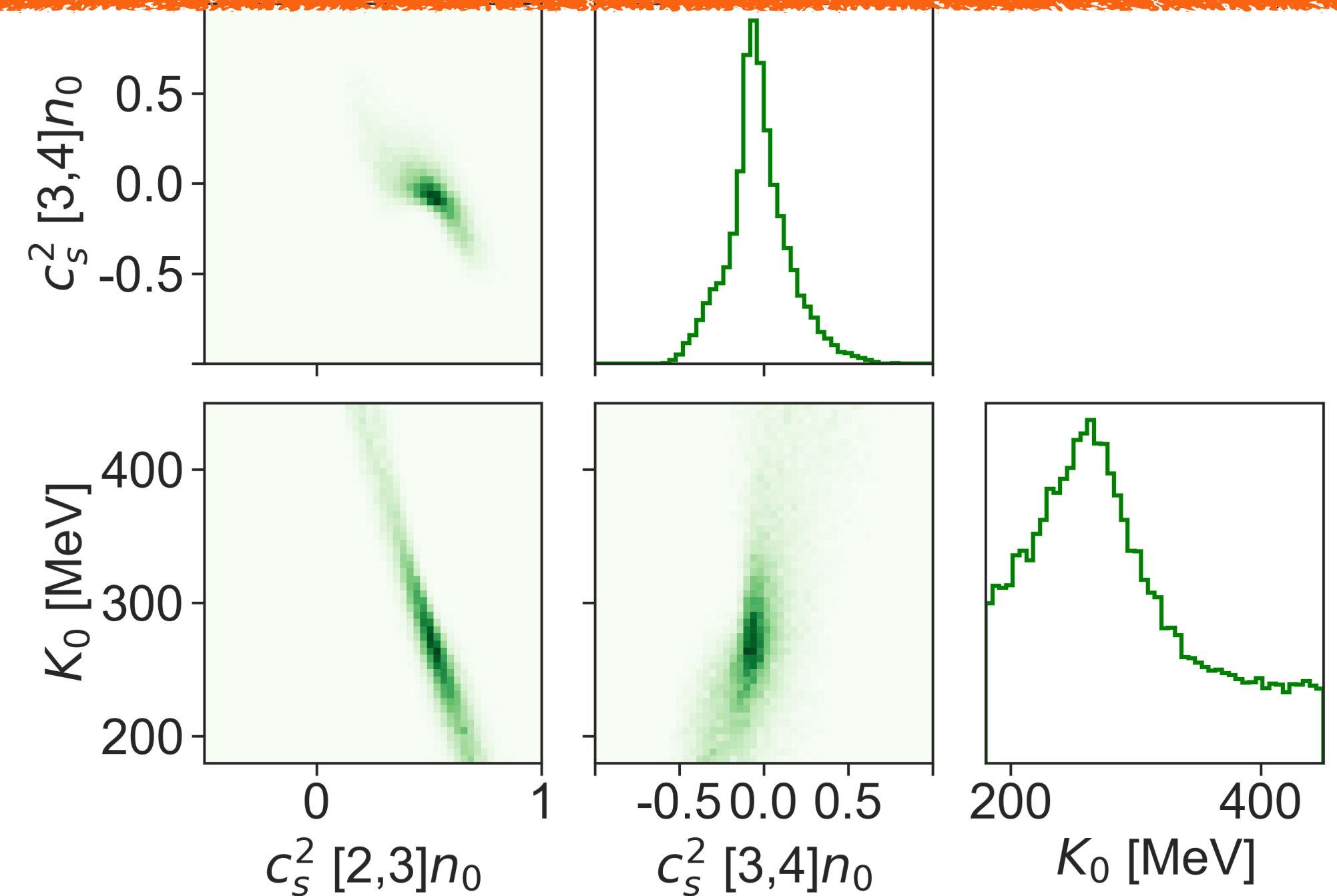
The maximum a posteriori probability (MAP) parameters are
 $K_0 = 285 \pm 67$ MeV, $c_{[2,3]n_0}^2 = 0.49 \pm 0.13$, $c_{[3,4]n_0}^2 = -0.03 \pm 0.15$

D. Oliinychenko, **A. Sorensen**, V. Koch, L. McLerran,
 Phys. Rev. C **108**, 3, 034908 (2023), arXiv:2208.11996

Bayesian analysis of BES flow in SMASH with varying K_0 , $c_{[2,3]n_0}^2$, $c_{[3,4]n_0}^2$



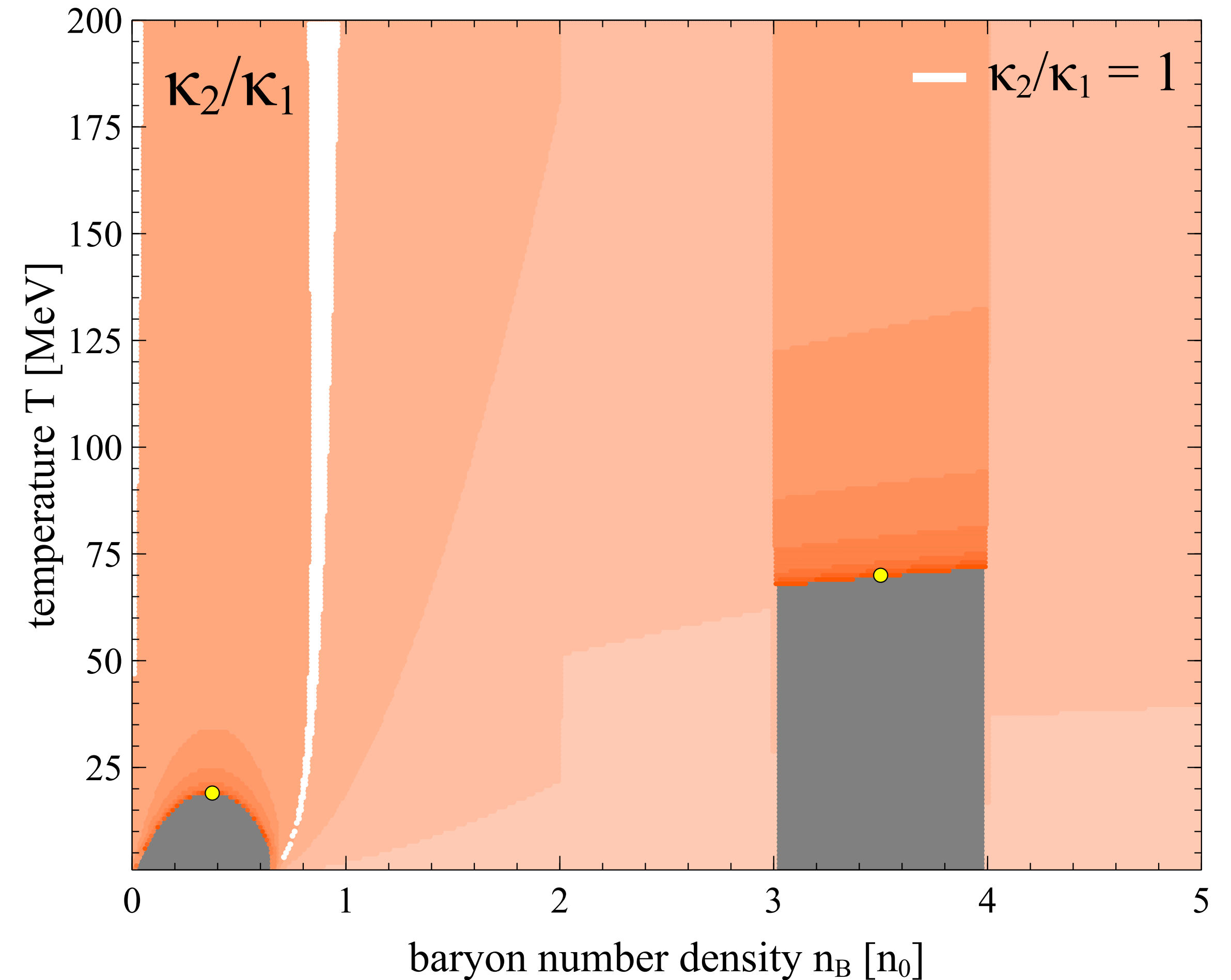
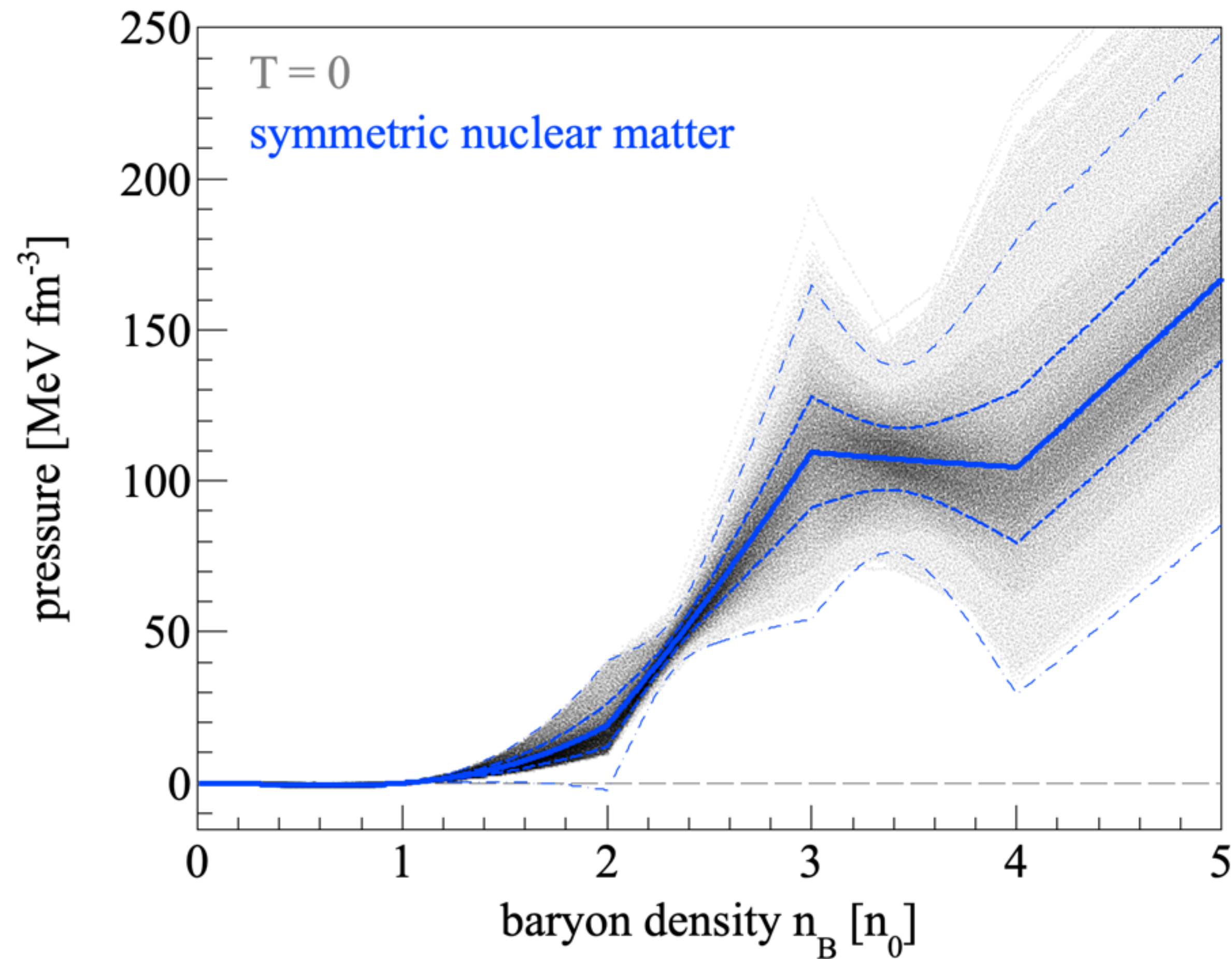
The constrained EOS is very stiff at $n_B \in (2,3)n_0$ and very soft at $n_B \in (3,4)n_0$



The maximum a posteriori probability (MAP) parameters are
 $K_0 = 285 \pm 67$ MeV, $c_{[2,3]n_0}^2 = 0.49 \pm 0.13$, $c_{[3,4]n_0}^2 = -0.03 \pm 0.15$

D. Oliinychenko, **A. Sorensen**, V. Koch, L. McLerran,
 Phys. Rev. C **108**, 3, 034908 (2023), arXiv:2208.11996

Bayesian analysis of BES flow in SMASH with varying K_0 , $c_{[2,3]n_0}^2$, $c_{[3,4]n_0}^2$

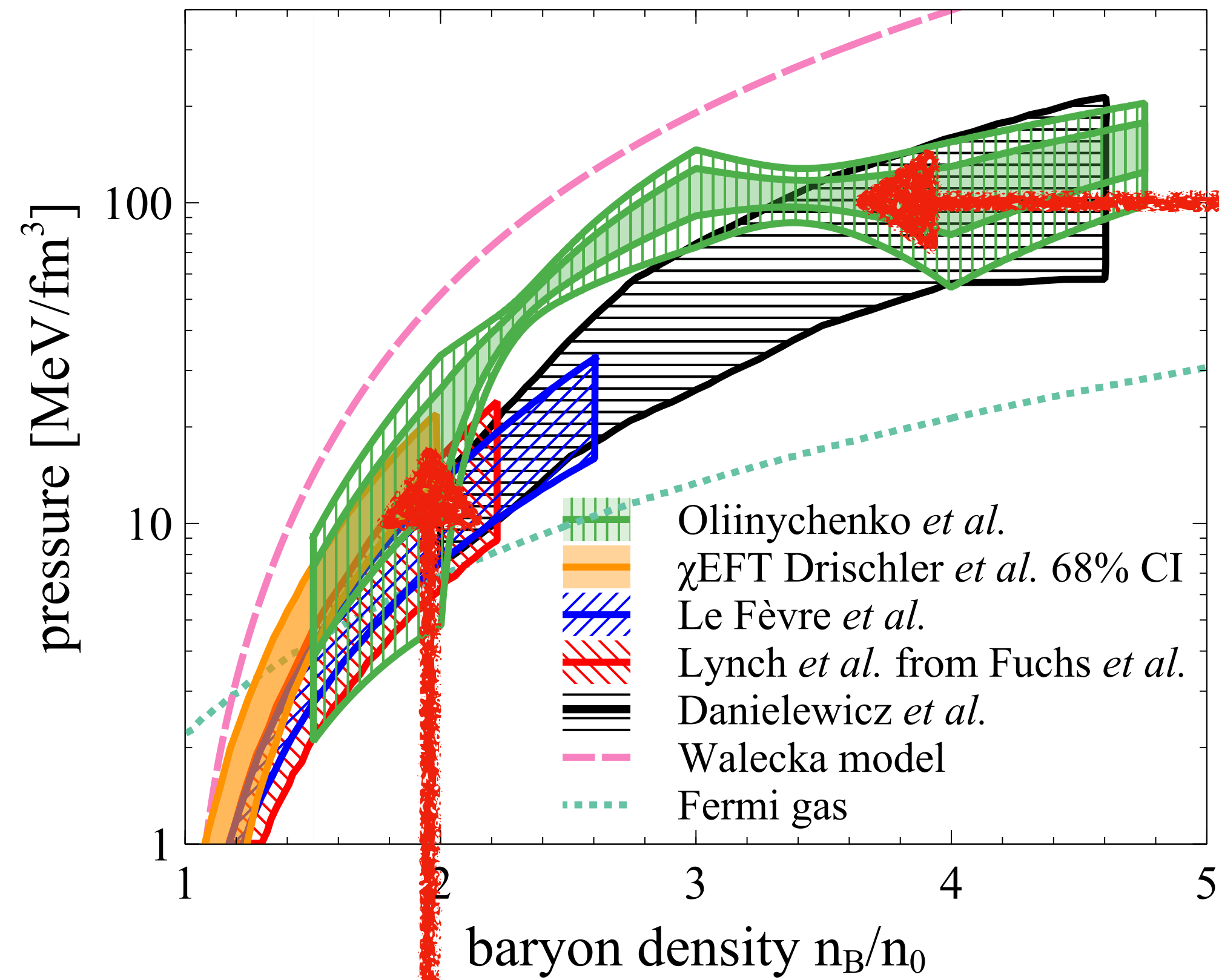


The maximum a posteriori probability (MAP) parameters are

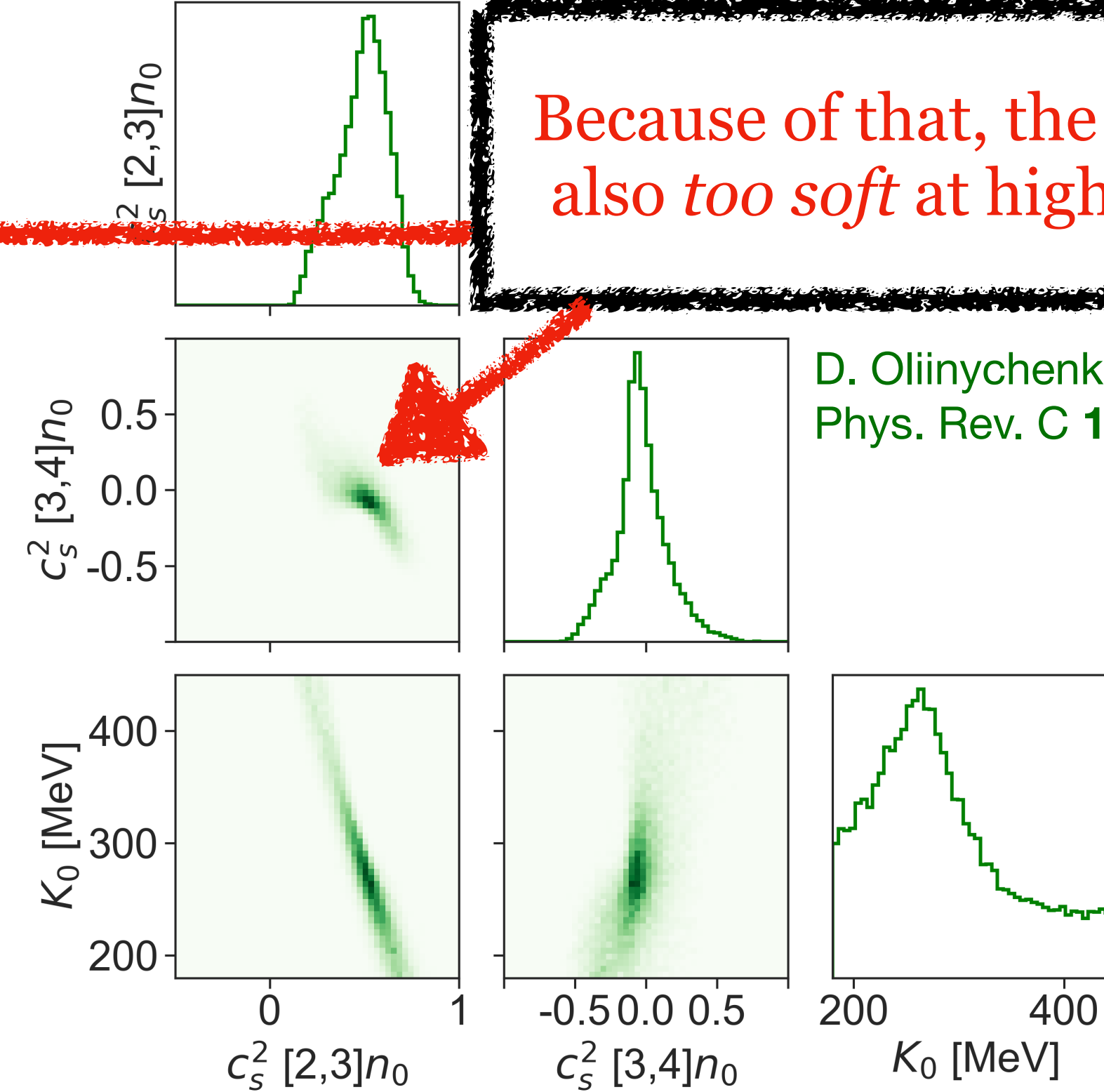
$$K_0 = 285 \pm 67 \text{ MeV}, \quad c_{[2,3]n_0}^2 = 0.49 \pm 0.13, \quad c_{[3,4]n_0}^2 = -0.03 \pm 0.15$$

D. Oliinychenko, A. Sorensen, V. Koch, L. McLerran, Phys. Rev. C **108**, 3, 034908 (2023), arXiv:2208.11996

Momentum-dependence of nuclear matter interactions



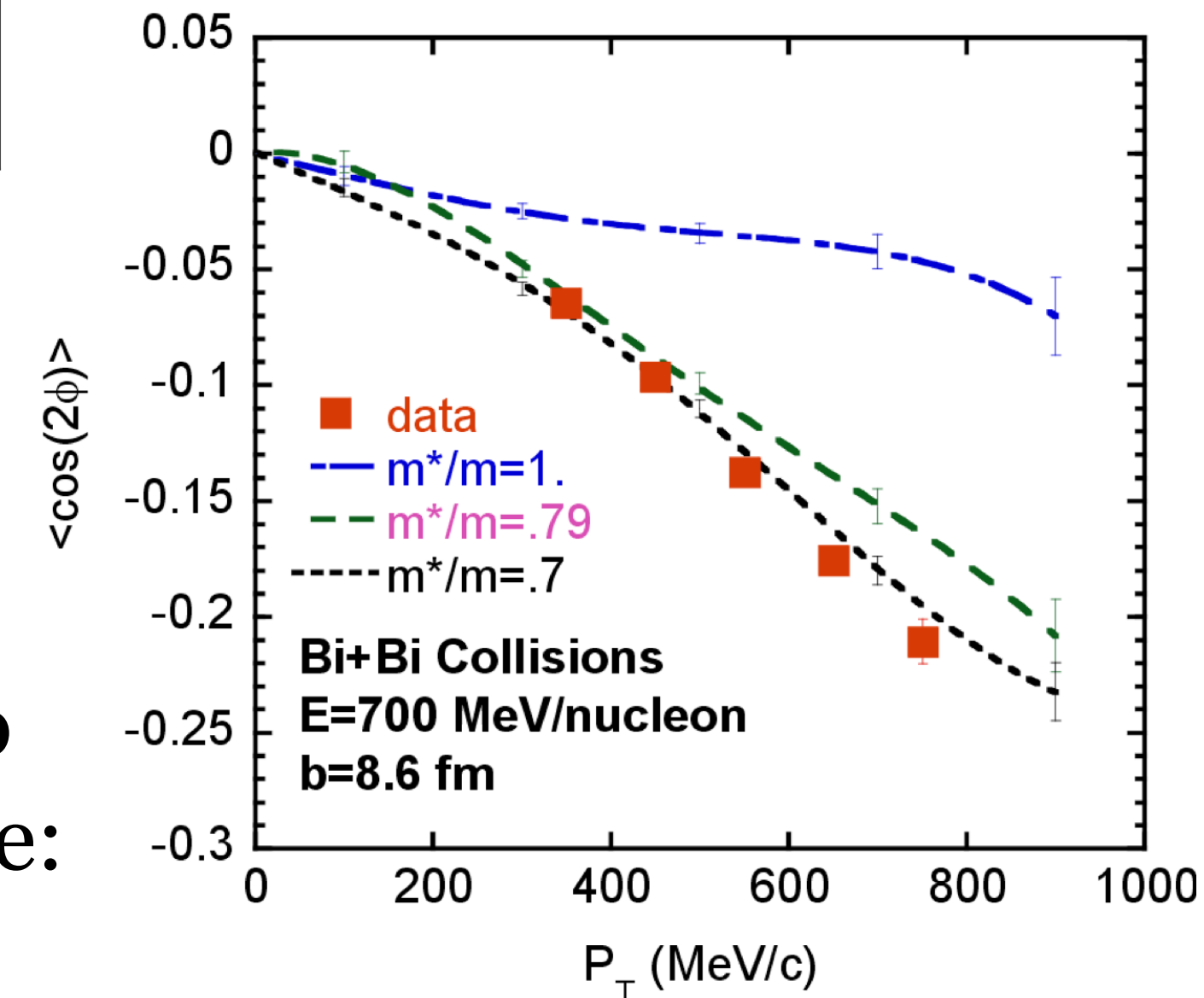
A. Sorensen *et al.*, Prog. Part. Nucl. Phys. **134**, 104080 (2024)
arXiv:2301.13253



Because of that, the EOS may be also *too soft* at higher densities

D. Oliinychenko, A. Sorensen, V. Koch, L. McLerran,
Phys. Rev. C **108**, 3, 034908 (2023), arXiv:2208.11996

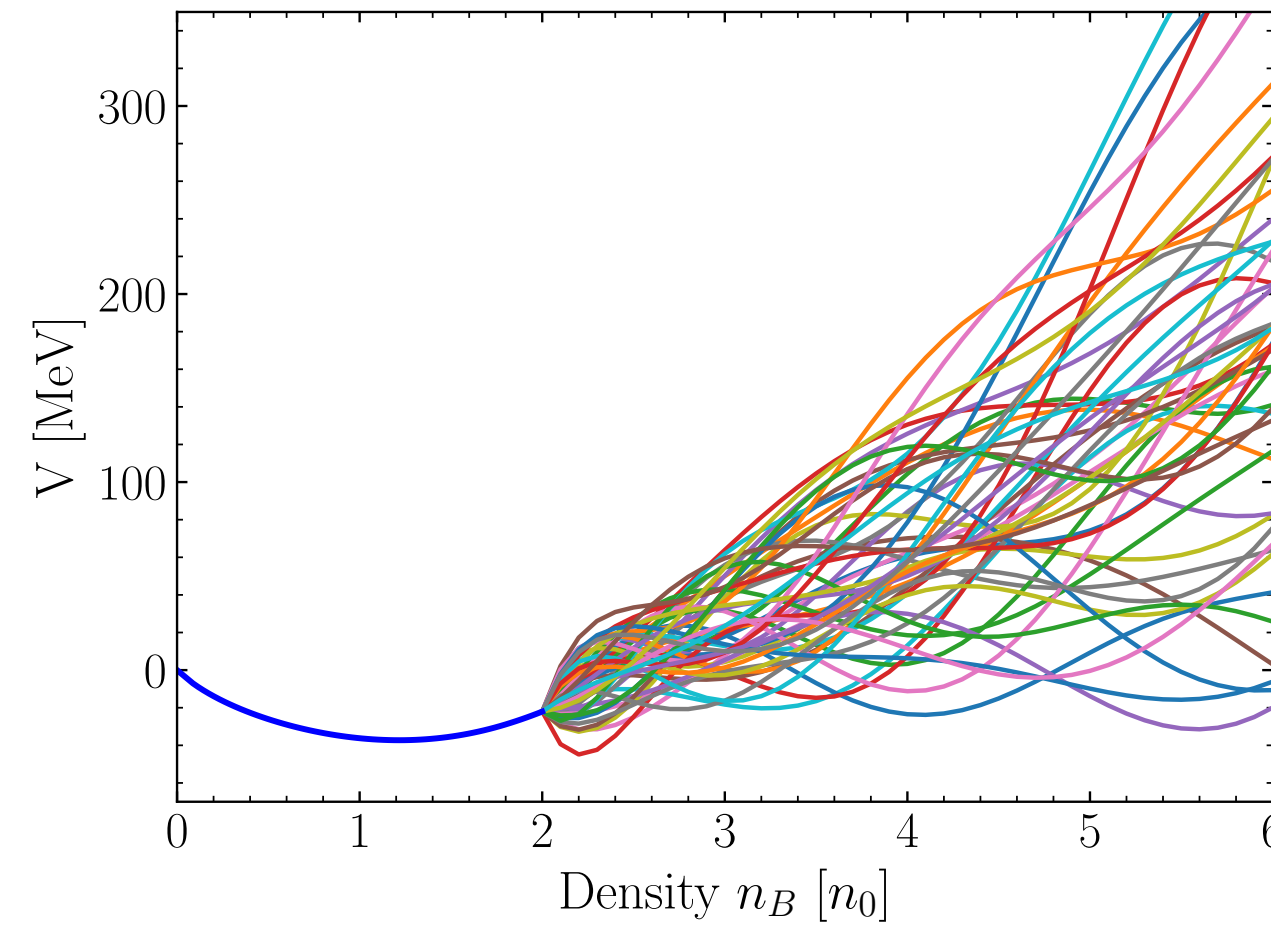
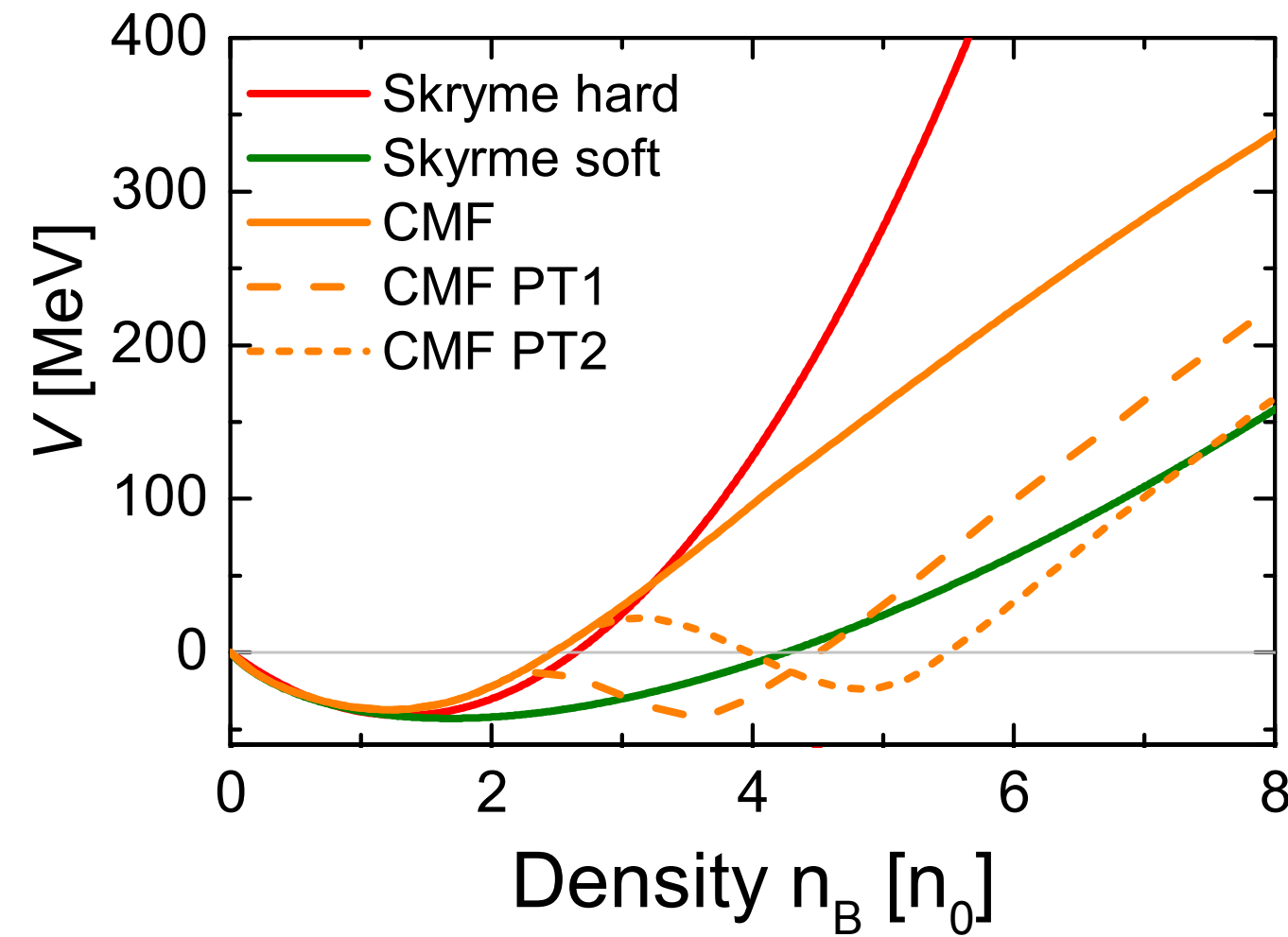
P. Danielewicz, R. Lacey, and W. G. Lynch,
Science **298**, 1592 (2002), arXiv:0208016



Use peripheral collisions to constrain the p -dependence:

Without momentum dependence, “artificial” additional source of repulsion is needed = the extracted EOS is too stiff?

Bayesian analysis of flow data in UrQMD



M. Omana Kuttan, J. Steinheimer, K. Zhou, H. Stoecker,
 Phys. Rev. Lett. **131** 20, 202303 (2023)
 arXiv:2211.11670

$$V(n_B) = \begin{cases} V_{\text{CMF}} & n_B \leq 2n_0 \\ \sum_{i=1}^7 \theta_i \left(\frac{n_B}{n_0} - 1\right)^i + C & n_B > 2n_0 \end{cases}$$

proton mean transverse kinetic energy $\langle m_T \rangle - m_0$:

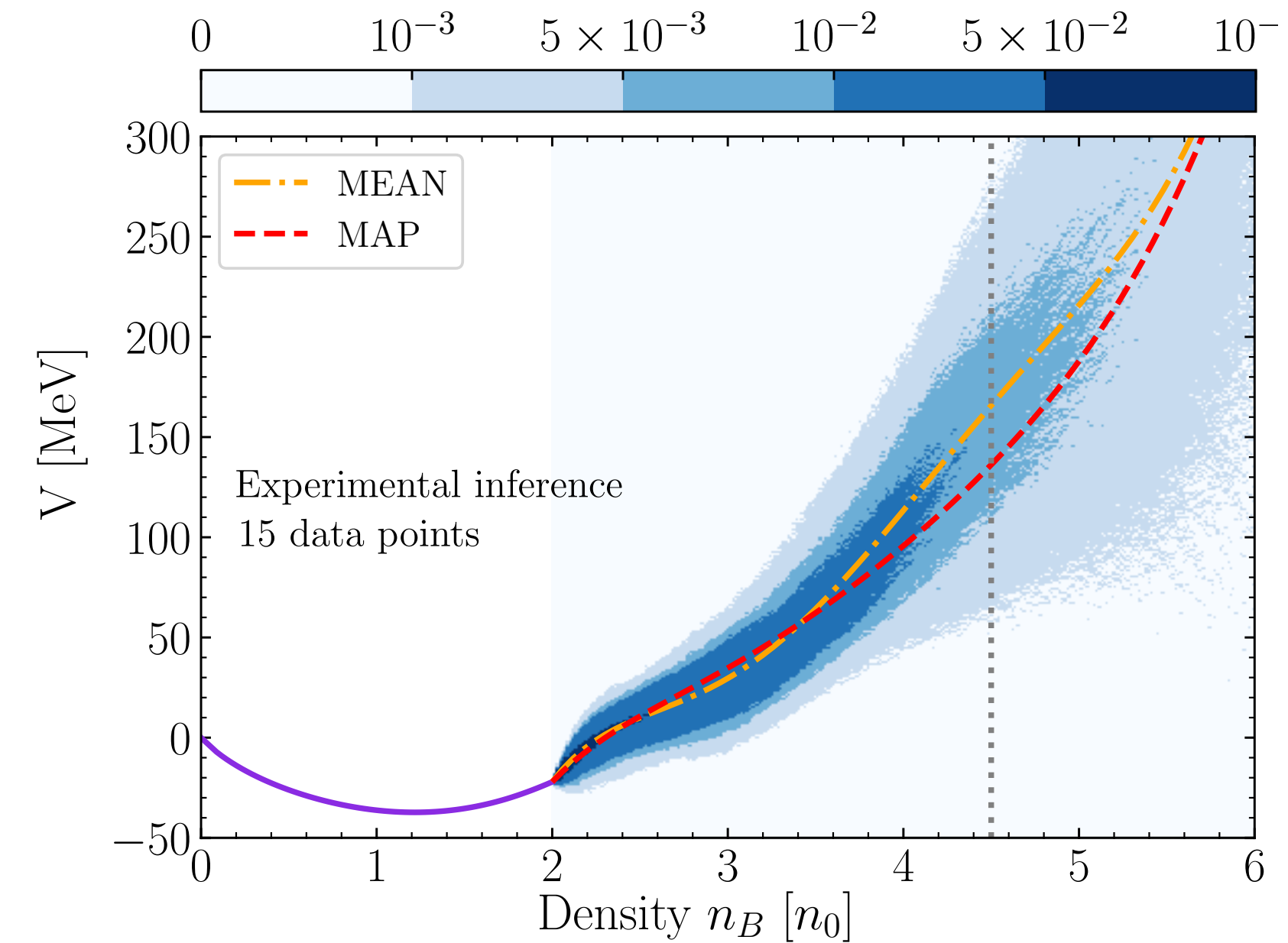
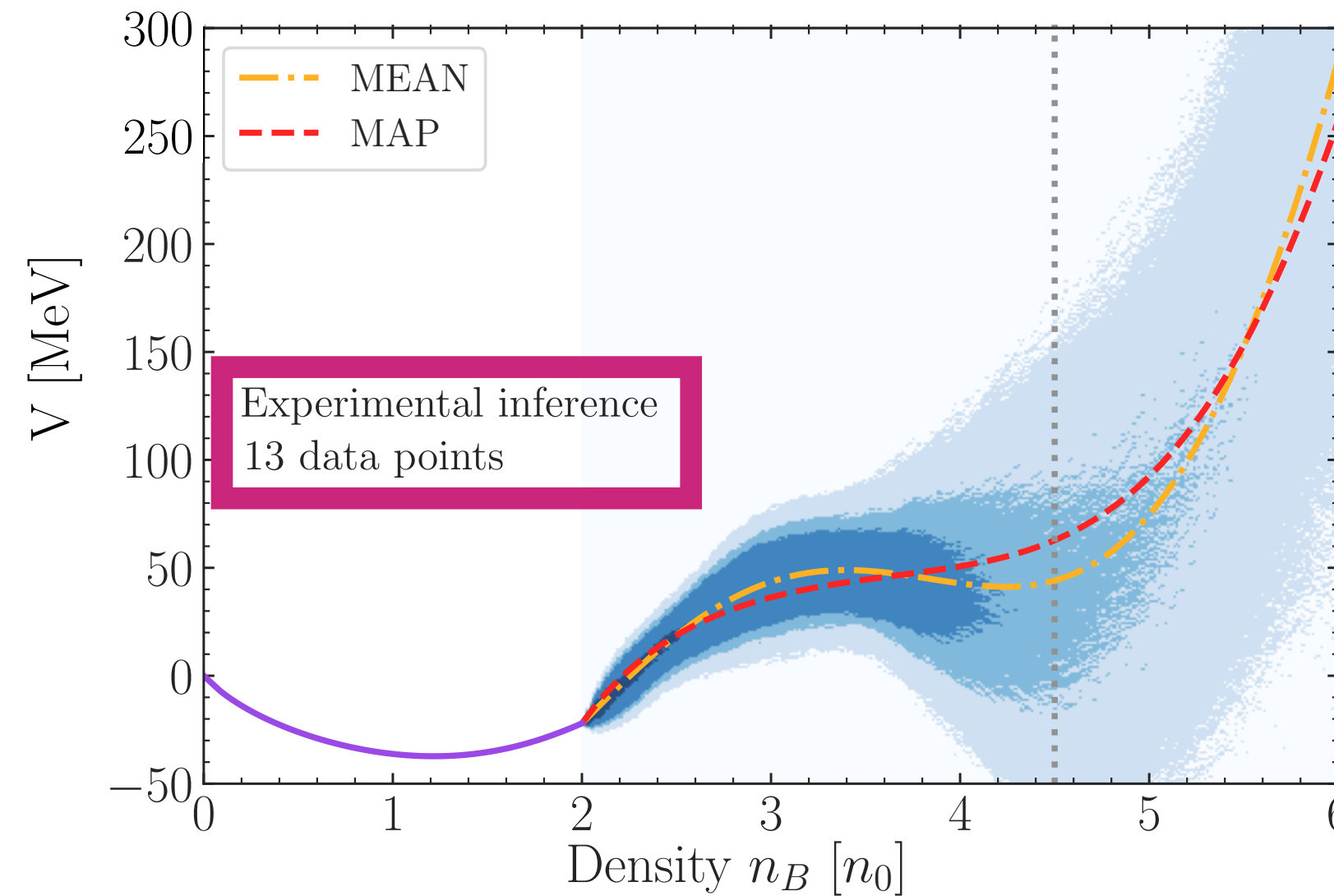
$$\sqrt{s_{\text{NN}}} \in [3.83, 8.86] \text{ GeV}$$

proton elliptic flow v_2 at midrapidity:

$$\sqrt{s_{\text{NN}}} \in [2.24, 4.72] \text{ GeV}$$

13 points = excluding $\langle m_T \rangle - m_0$
 at the two lowest collision energies

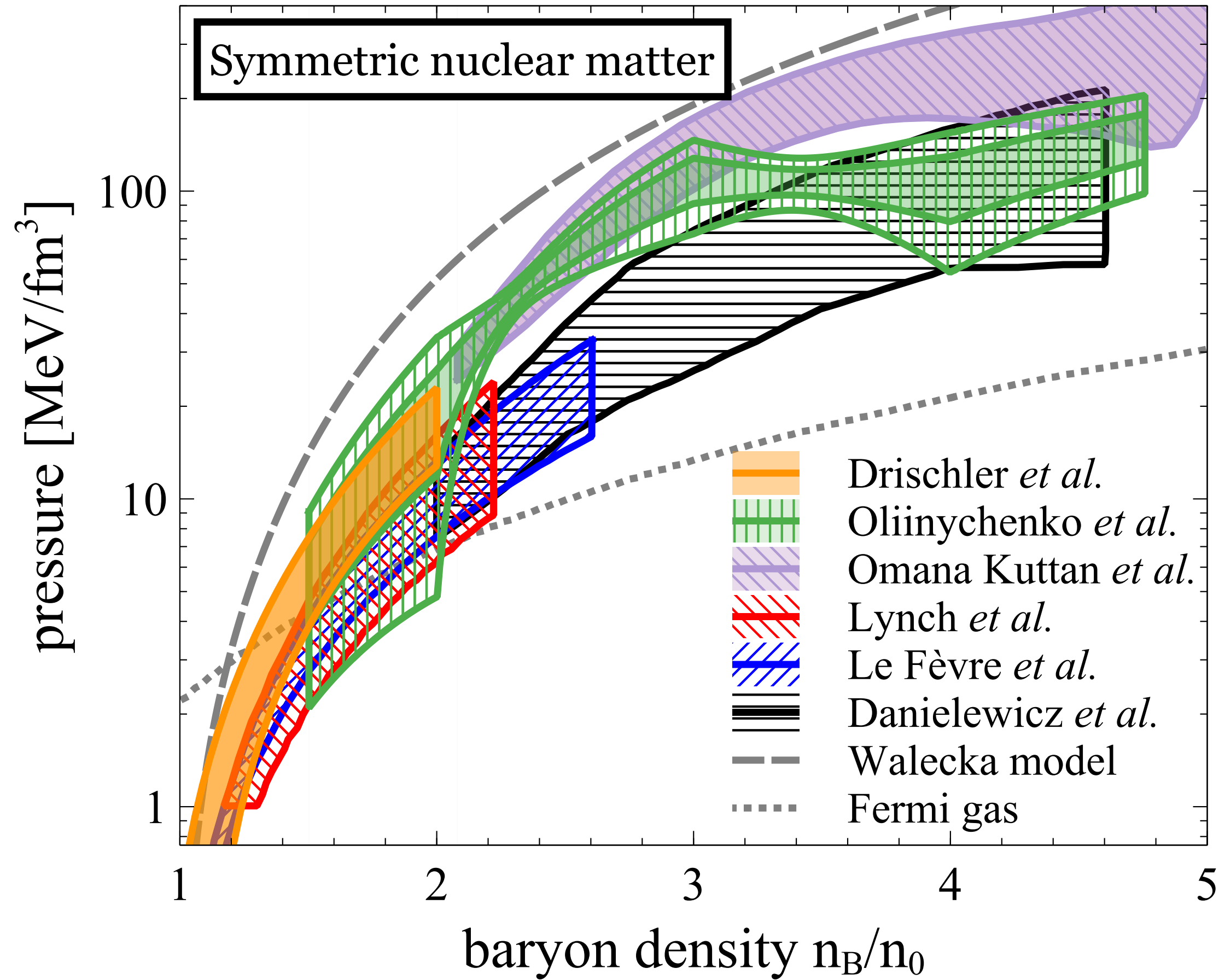
$$(\sqrt{s_{\text{NN}}} = 3.83, 4.29 \text{ GeV})$$



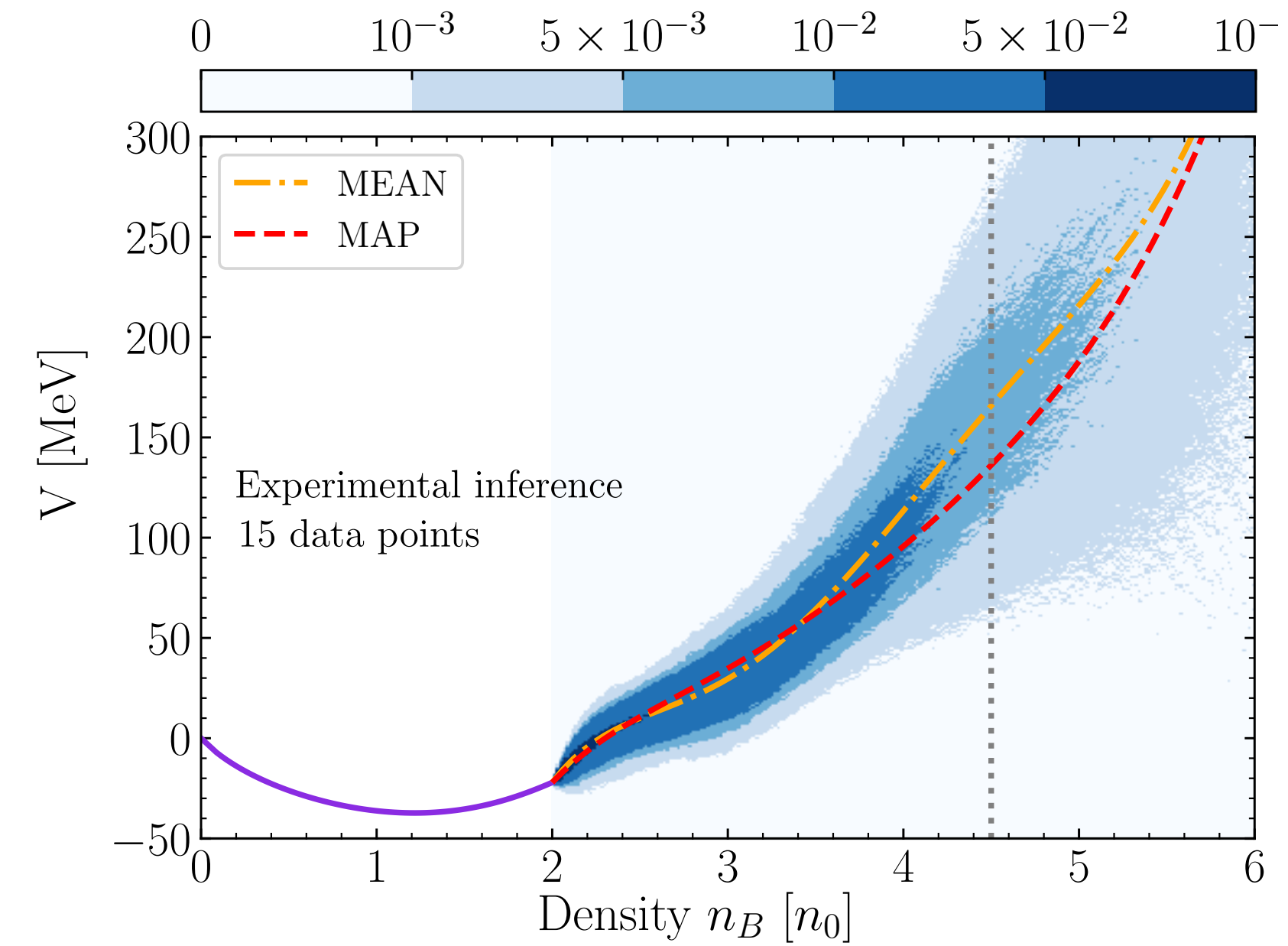
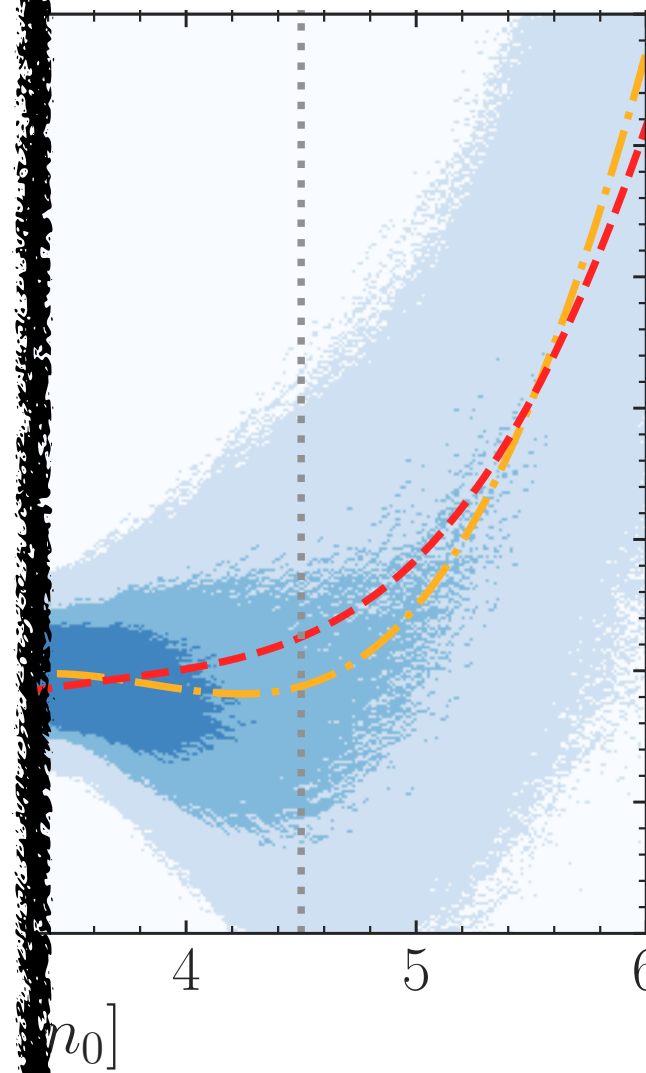
Bayesian analysis of flow data in UrQMD

M. Omana Kuttan, J. Steinheimer, K. Zhou, H. Stoecker,
 Phys. Rev. Lett. **131** 20, 202303 (2023)
 arXiv:2211.11670

$$V(n_B) = \begin{cases} V_{\text{CMF}} & n_B \leq 2n_0 \\ \sum_{i=1}^7 \theta_i \left(\frac{n_B}{n_0} - 1\right)^i + C & n_B > 2n_0 \end{cases}$$

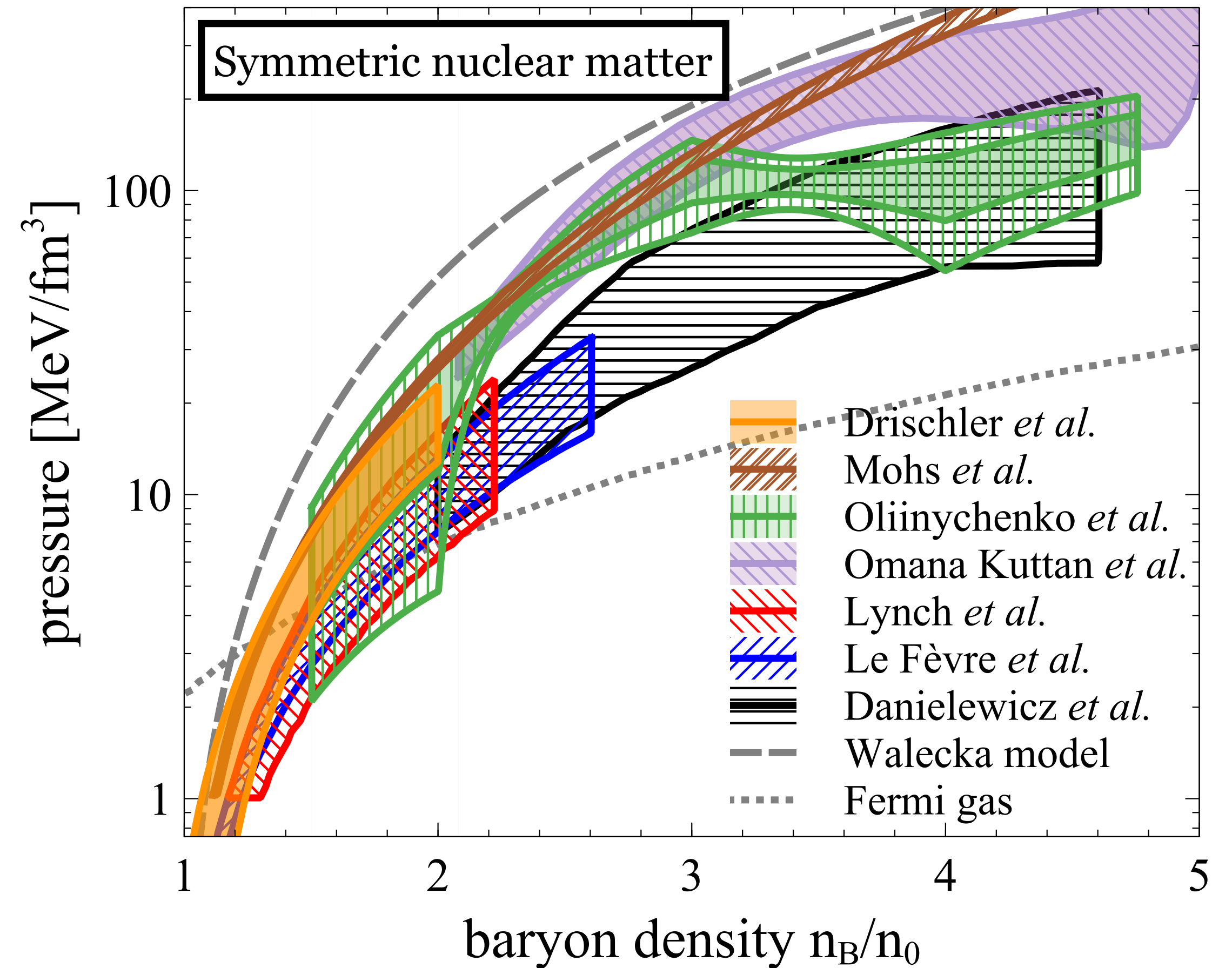
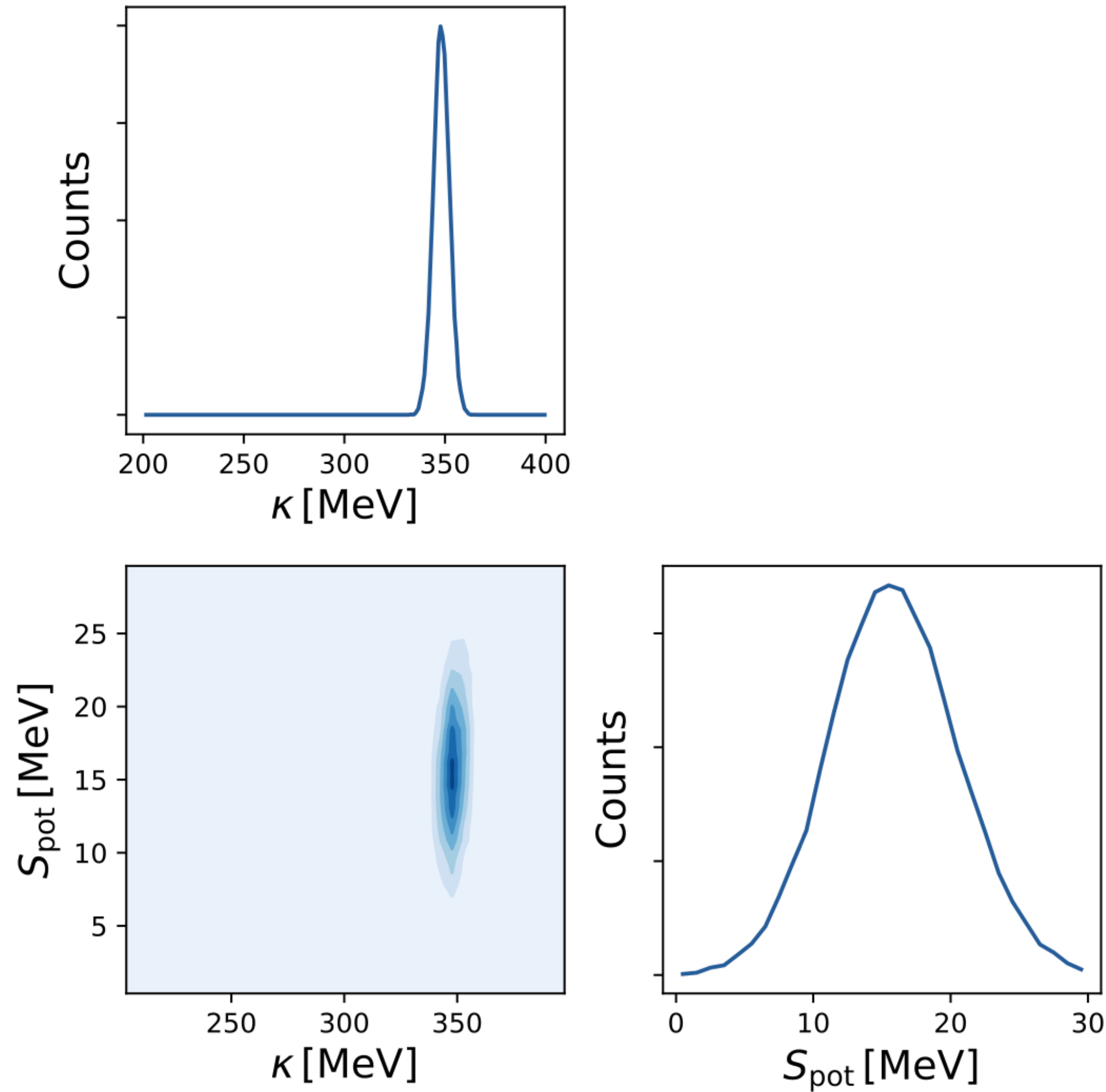


L. Du, A. Sorensen, M. Stephanov, Int. J. Mod. Phys. E **33** (2024)
 07, 2430008, arXiv: 2402.10183



Just in: Bayesian analysis of HADES flow in SMASH

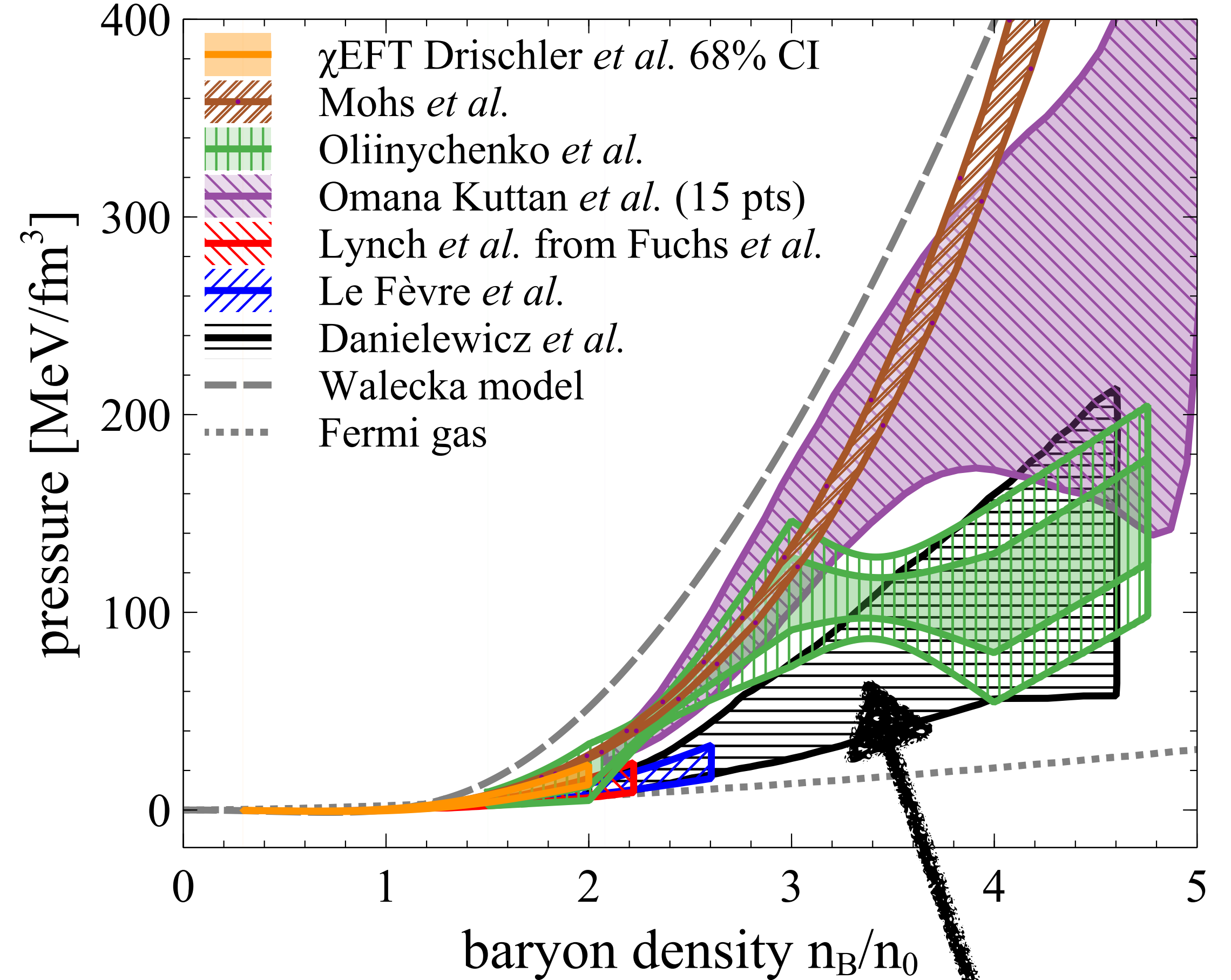
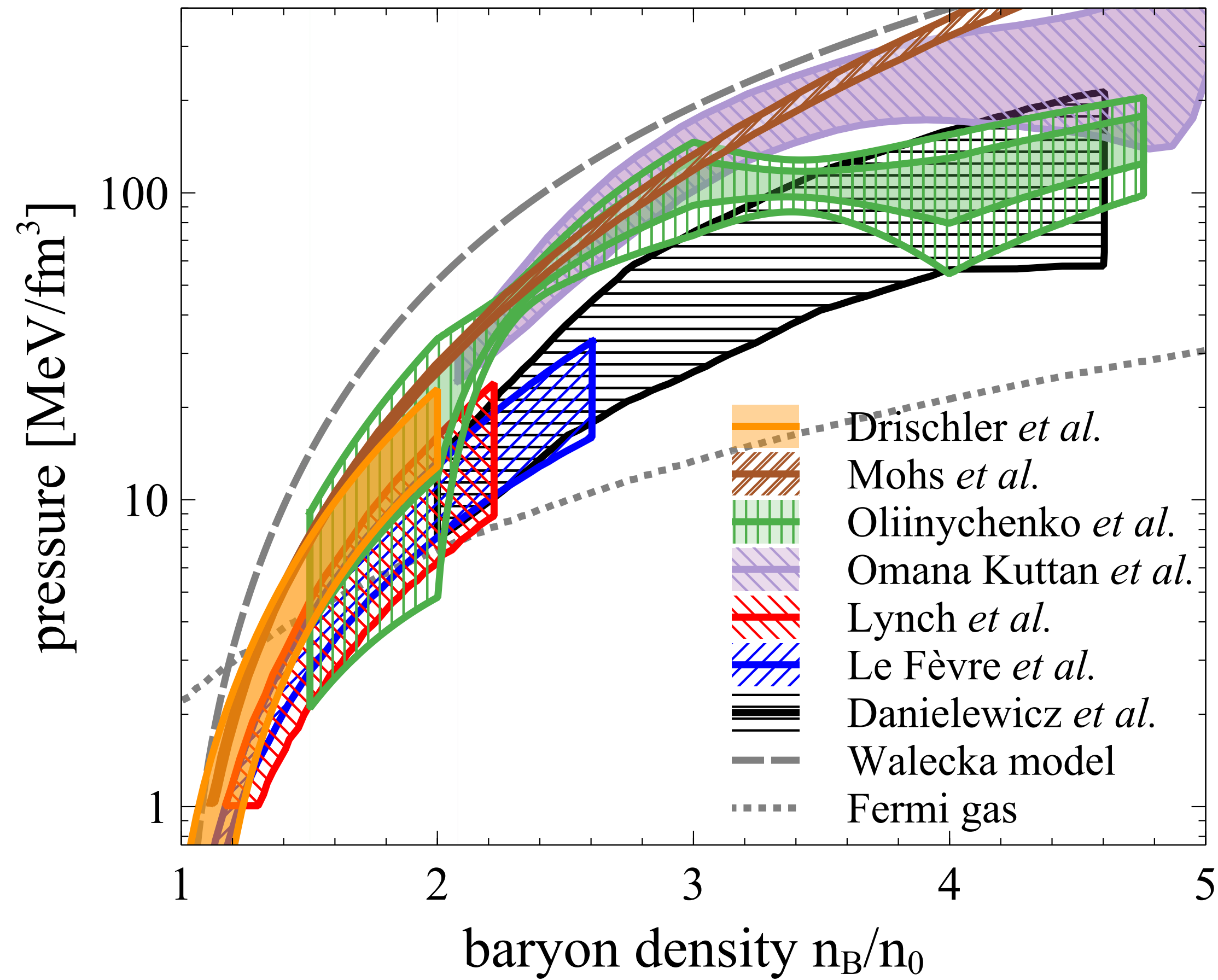
EOS: Skyrme-like with momentum dependence*



L. Du, **A. Sorensen**, M. Stephanov, *Int. J. Mod. Phys. E* 33 (2024) 07, 2430008, arXiv: 2402.10183

J. Mohs, S. Spies, H. Elfner, arXiv:2409.16927

EOS of symmetric nuclear matter: *selected* new results



possible phase transition
at $n_B \in (3,4)n_0$

D. Oliinychenko, A. Sorensen, V. Koch, L. McLerran, Phys. Rev. C **108**, 3, 034908 (2023), arXiv:2208.11996

M. Omana Kuttan, J. Steinheimer, K. Zhou, H. Stoecker, Phys. Rev. Lett. **131** 20, 202303 (2023), arXiv:2211.11670

J. Mohs, S. Spies, H. Elfner, arXiv:2409.16927

Finite-size scaling results

Universal behavior

Near CP:

$$c_\infty(t,0) \sim |t|^{-\alpha}$$

$$\chi_\infty(t,0) \sim |t|^{-\gamma}$$

$$\xi_\infty(t,0) \sim |t|^{-\nu}$$

$$\xi_\infty(0,h) \sim |h|^{-\nu_c}$$

$$t \equiv \frac{T - T_c}{T_c}$$

$$h \equiv \frac{H}{k_B T}$$

For a thermodynamic quantity $X \sim |t|^{-\sigma}$: $X_\infty(t) \sim |t|^{-\sigma} \sim [\xi_\infty(t)]^{\frac{\sigma}{\nu}}$

Scaling is not unique to critical phenomena.

Scaling law = a physical quantity changes predictably with the scaling of another quantity

E.g., Kepler's third law:

The orbital period of a planet scales as the cube of the semi-major axis of its orbit:

$$P^2 = a^3$$

The important question for scaling is: **what is the scale relevant to the problem?**

Universal behavior

Near CP:

$$c_{\infty}(t,0) \sim |t|^{-\alpha}$$

$$\chi_{\infty}(t,0) \sim |t|^{-\gamma}$$

$$\xi_{\infty}(t,0) \sim |t|^{-\nu}$$

$$\xi_{\infty}(0,h) \sim |h|^{-\nu_c}$$

$$t \equiv \frac{T - T_c}{T_c}$$

$$h \equiv \frac{H}{k_B T}$$

For a thermodynamic quantity $X \sim |t|^{-\sigma}$: $X_{\infty}(t) \sim |t|^{-\sigma} \sim [\xi_{\infty}(t)]^{\frac{\sigma}{\nu}}$

CP: infinite volume concept

In real world ξ does not go to infinity = thermodynamic functions do not exhibit singularities

ξ is bound by the size of the system $L \Rightarrow X_L(t_L) \sim L^{\frac{\sigma}{\nu}}$

$$\Rightarrow X_L(t_L) = L^{\frac{\sigma}{\nu}} \phi(t, L) = L^{\frac{\sigma}{\nu}} \phi(tL^{\frac{1}{\nu}})$$

$$\Rightarrow X_L(t_L) L^{-\frac{\sigma}{\nu}} = \phi(tL^{\frac{1}{\nu}})$$

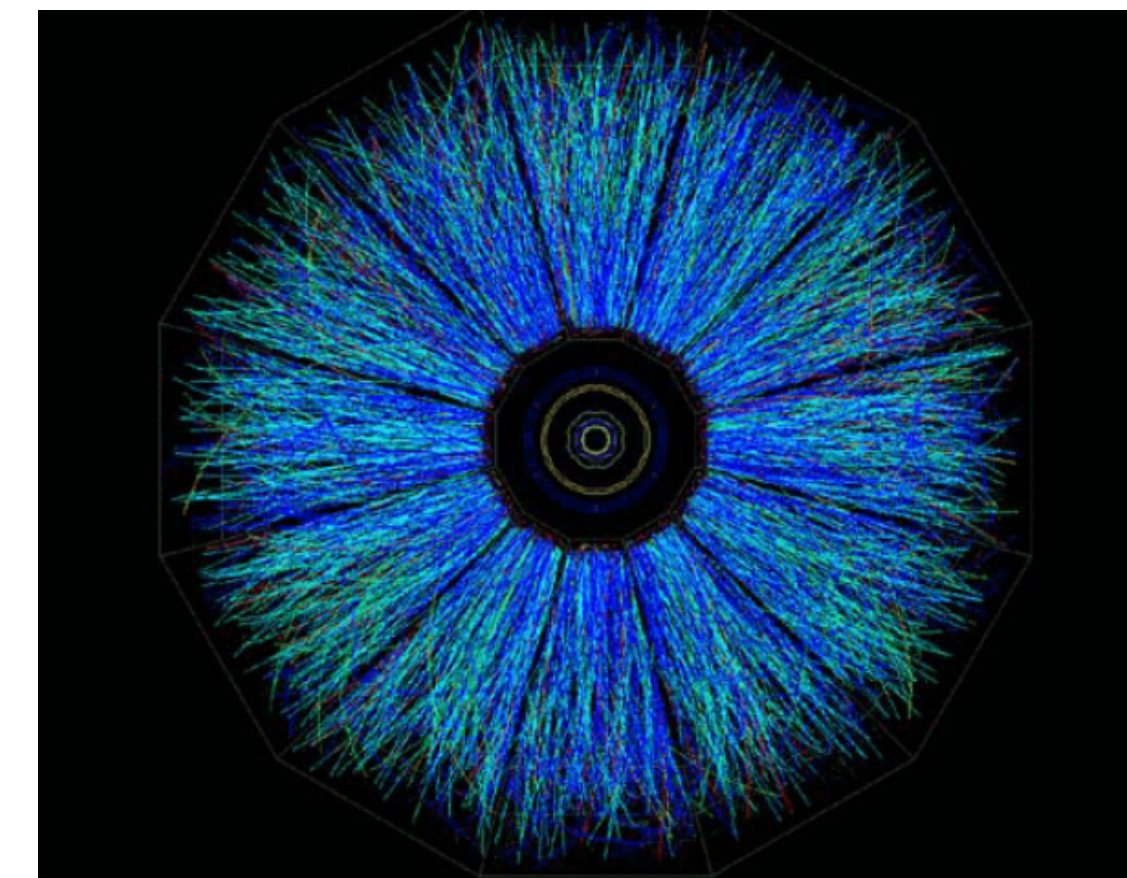
one can find CP by plotting

Finite size vs. window size

$$X_L(t_L)L^{-\frac{\sigma}{\nu}} = \phi(tL^{\frac{1}{\nu}})$$

Finite-size scaling: change the size of the system, calculate $X_L(t_L)$, repeat

However, changing SIZE is not always possible or doesn't probe the same system:
bird flocks, heavy-ion collisions, ...



Solution: study the dependence of X on the size of the *subsystem* that is considered

D. Martin, T. Ribeiro, S. Cannas, *et al.*, Box scaling as a proxy of finite size correlations, Sci Rep 11, 15937 (2021)

THIS WORK: the size of the *subsystem* = rapidity bin width W

A. Sorensen, P. Sorensen, arXiv:2405.10278

Thermal model

- We consider finite-size scaling of proton number susceptibility:

$$\chi_2 = \frac{C_2}{T^3 V} \quad \Rightarrow \quad \chi_2(W, \mu_{f_0}) = \frac{C_2(W, \mu_{B,f_0})}{T_{f_0}^3 W dV_{f_0}/dy}$$

- We use **rapidity bin width W** as the subsystem size
- We use published thermal model fits for T_{f_0} and μ_{B,f_0}
- We parameterize dV_{f_0}/dy from several publications (for 2.4 GeV, $T_{f_0}^3 V$ is highly uncertain, ranging from about 65 to 650)
- Experiments can improve results** by publishing $dV_{f_0}/dy, T_{f_0}, \mu_{B,f_0}$ **from thermal model fits for specific W**

$\sqrt{s_{NN}}$ (GeV)	y_{beam}	μ_{f_0} (GeV)	T_{f_0} (GeV)	dV_{f_0}/dy (fm ³)
2.4	0.73	0.776	0.050	17157
3.0	1.05	0.720	0.080	4850
7.7	2.09	0.398	0.144	1044
11.5	2.50	0.287	0.149	1047
14.5	2.73	0.264	0.152	1080
19.6	3.04	0.188	0.154	1137
27	3.36	0.144	0.155	1218
39	3.73	0.103	0.156	1341
54.4	4.06	0.083	0.160	1487

J. Adamczewski-Musch et al. (HADES), Phys. Rev. C 102, 024914 (2020)

M. Abdallah et al. (STAR), Phys. Rev. C 104, 024902 (2021)

M. Abdallah et al. (STAR), Phys. Rev. C 107, 024908 (2023)

A. Andronic, P. Braun-Munzinger, J. Stachel, Acta Phys. Polon. B 40, 1005-1012 (2009)

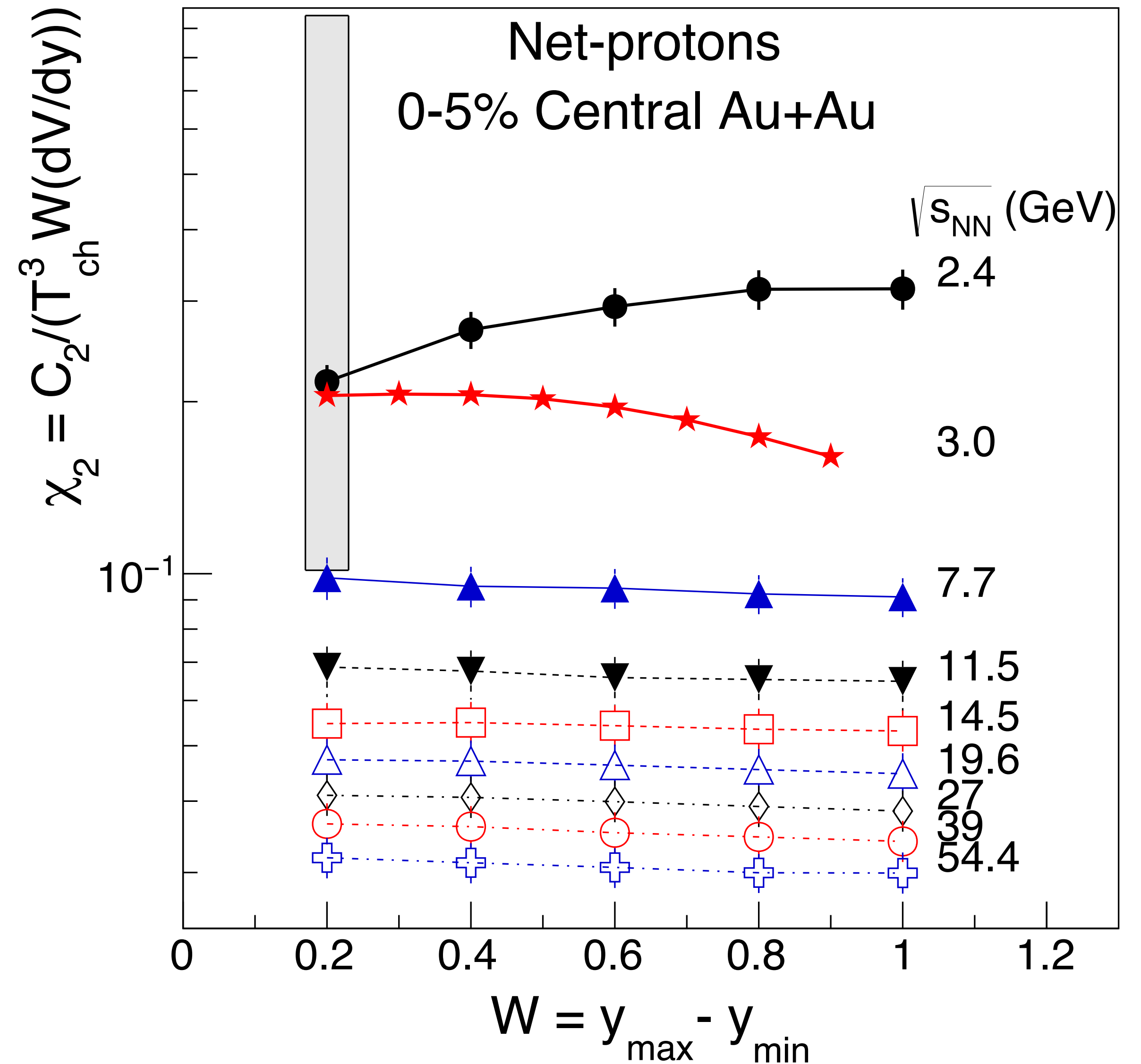
A. Motornenko et al., Phys. Lett. B 822, 136703 (2021)

S. Chatterjee et al., Adv. High Energy Phys. 2015, 349013 (2015)

Susceptibility results

$$\chi_2(W, \mu_{fo}) = \frac{C_2(W, \mu_{B,fo})}{T_{fo}^3 W dV_{fo}/dy}$$

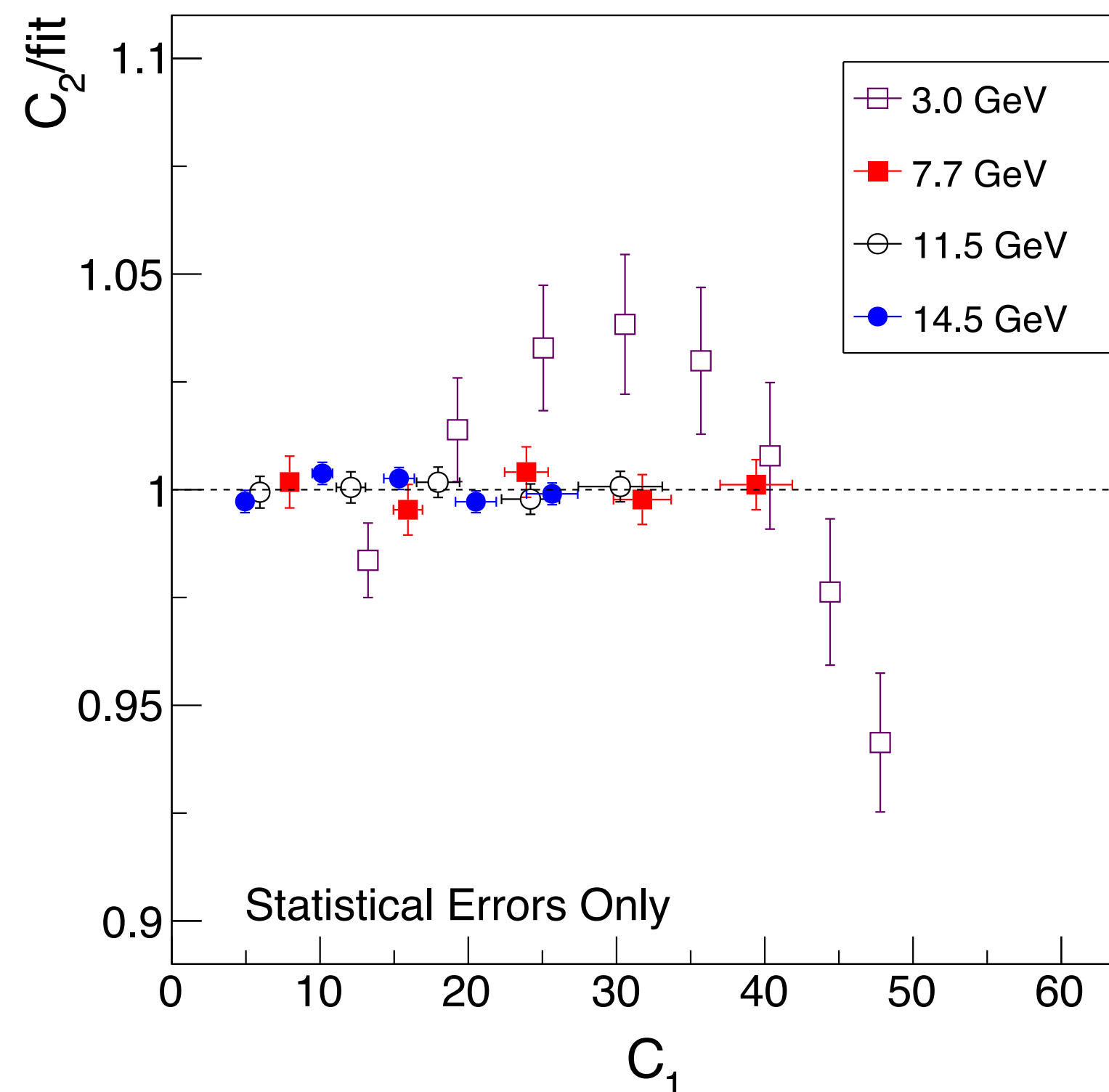
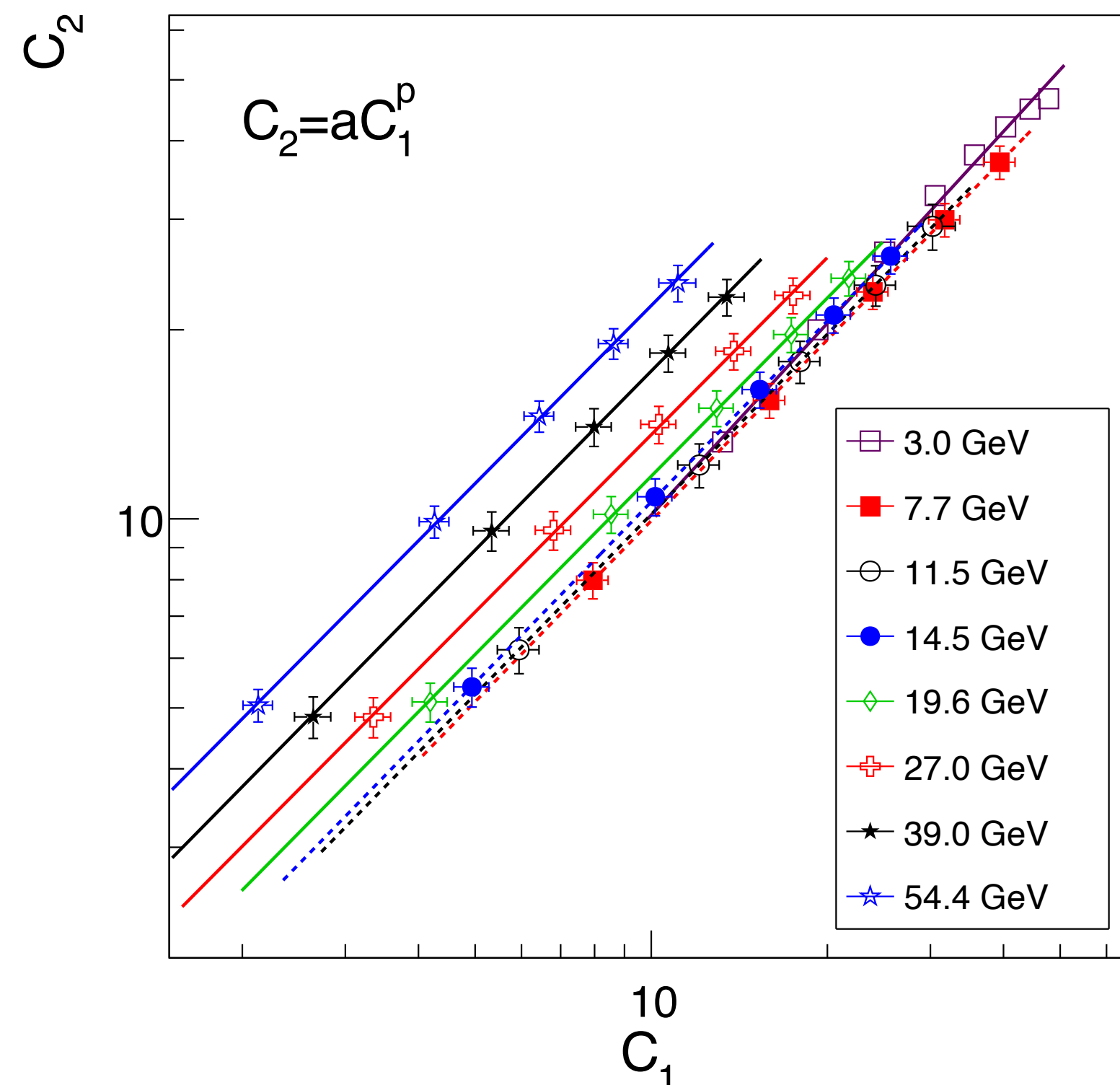
- Grey band shows uncertainty from freeze-out ambiguities for the 2.4 GeV data.
Uncertainty precludes any conclusion about observing a maximum in χ_2
 (with a critical point, you should see a maximum in χ_2)



Where can we expect scaling behavior?

- For fluids far from the critical region, a mean-field treatment is good enough. The transition between the critical scaling region, intermediate scaling region, and extended scaling region has been studied: for fluids, the extended scaling region essentially covers the entire phase diagram where fluctuation contributions are small but finite.

M.A. Anisimov, S.B. Kiselev, J.V. Sengers, S.Tang, Crossover approach to global critical phenomena in fluids, Physica A 188, 4 (1992)
- In the region of the phase diagram where the bulk of the evolution is well described by hydrodynamics (a scale free theory for $\eta \approx 0$), the data follows Taylor's Law: $\sigma^2 = a\lambda^p$ (scale free)



$$C_2 = aW^p$$

$$C_2 = a(xW)^p = ax^pW^p = a'W^p$$

where $C_1 \propto W$ in this energy range

Scale invariance supports the applicability of FSS for $\sqrt{s_{NN}} \geq 7.7$ GeV

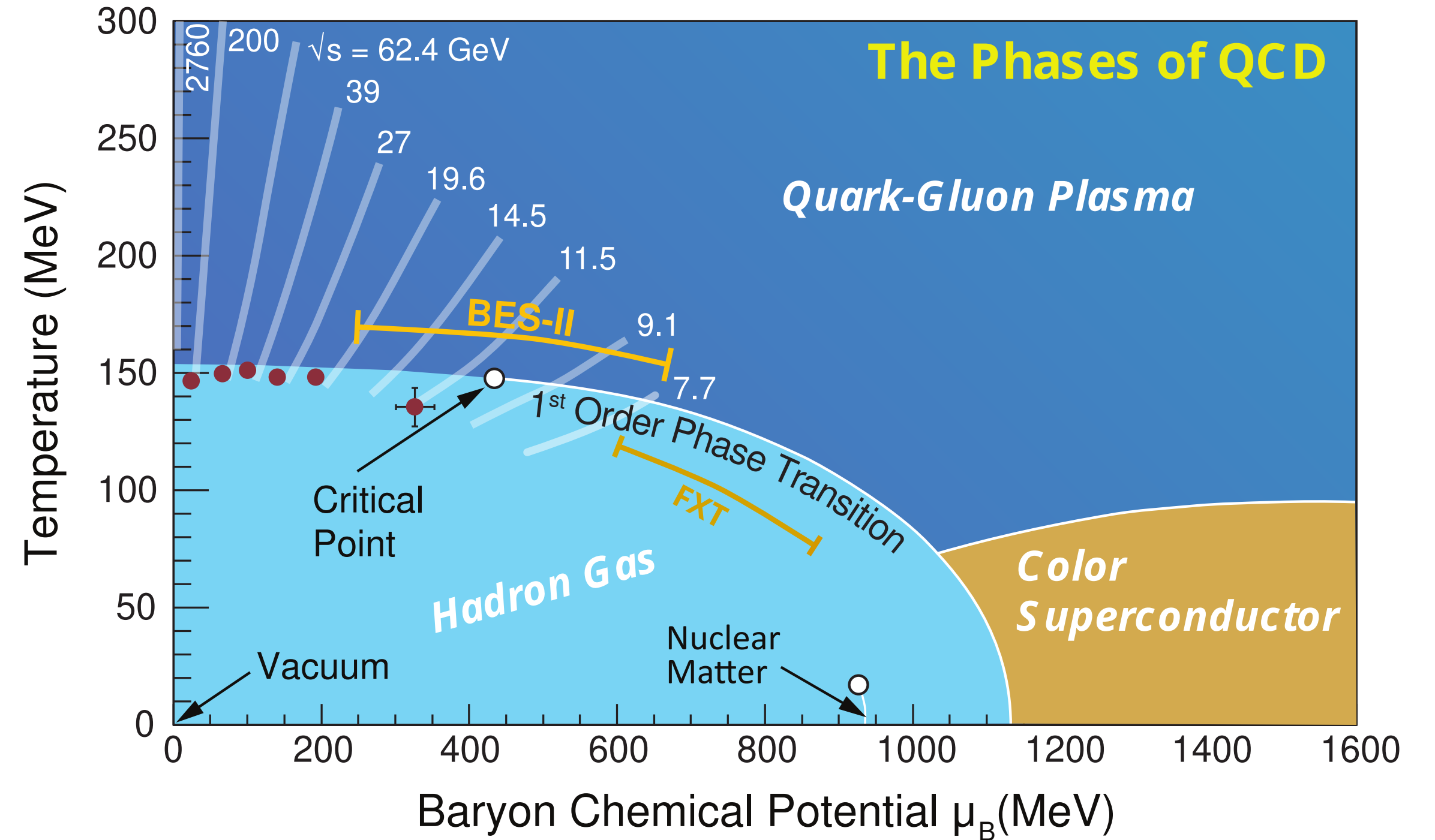
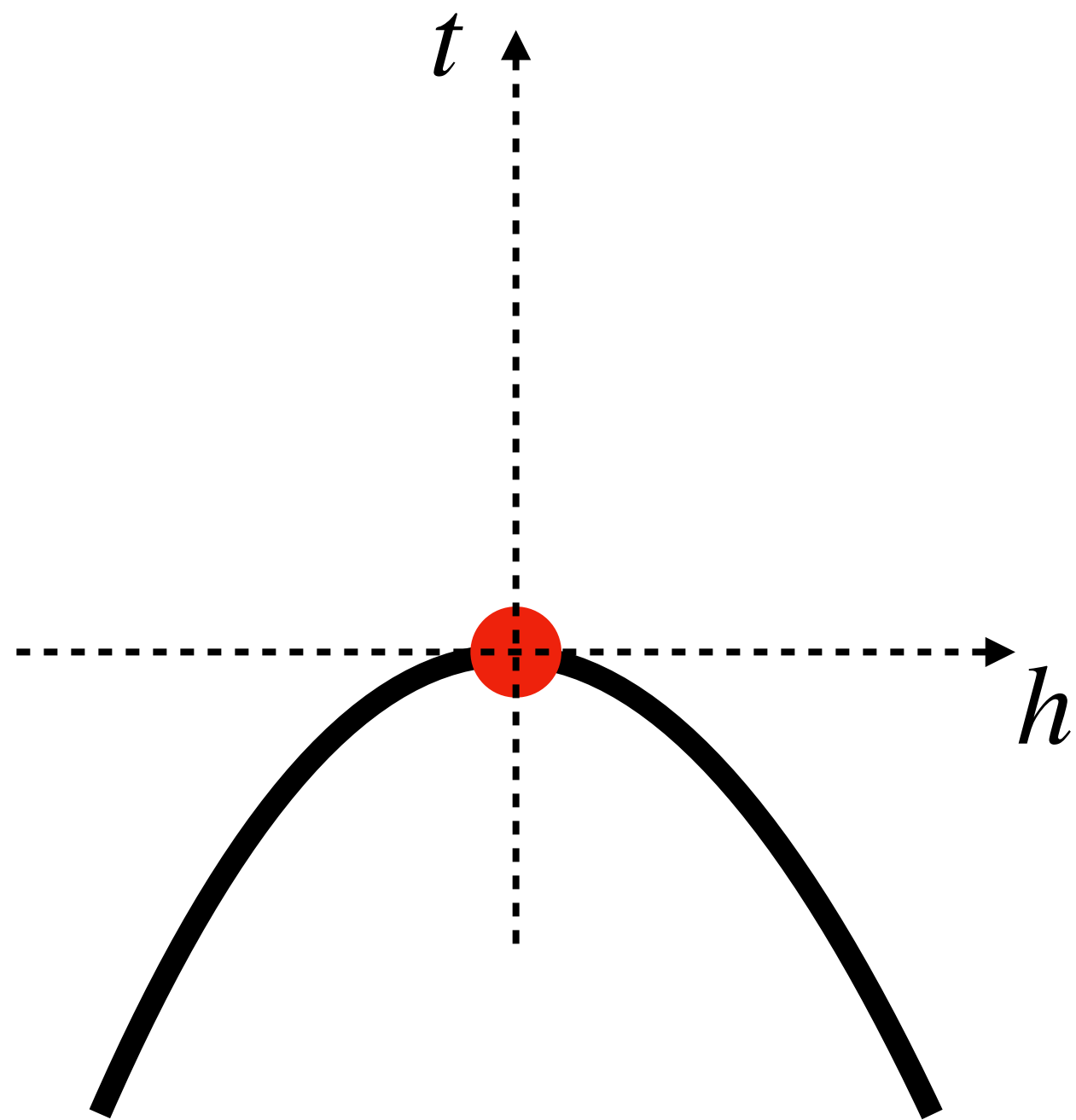
What to scale with?

$$\xi_\infty(t,0) \sim |t|^{-\nu}$$

$$\xi_\infty(0,h) \sim |h|^{-\nu_c}$$

$$t \equiv \frac{T - T_c}{T_c}$$

$$h \equiv \frac{H}{k_B T}$$



$$X_L(t_L)L^{-\frac{\sigma}{\nu}} = \phi(tL^{\frac{1}{\nu}})$$

one can find CP by plotting

$$h(\mu, T) = - \frac{\cos \alpha_1 \Delta T + \sin \alpha_1 \Delta \mu}{w T_c \sin(\alpha_1 - \alpha_2)}$$

$$t(\mu, T) = \frac{\cos \alpha_2 \Delta T + \sin \alpha_2 \Delta \mu}{\rho w T_c \sin(\alpha_1 - \alpha_2)}$$

M.S. Pradeep, M. Stephanov, Phys. Rev. D **100**
5, 056003 (2019) arXiv:1905.13247

What to scale with?

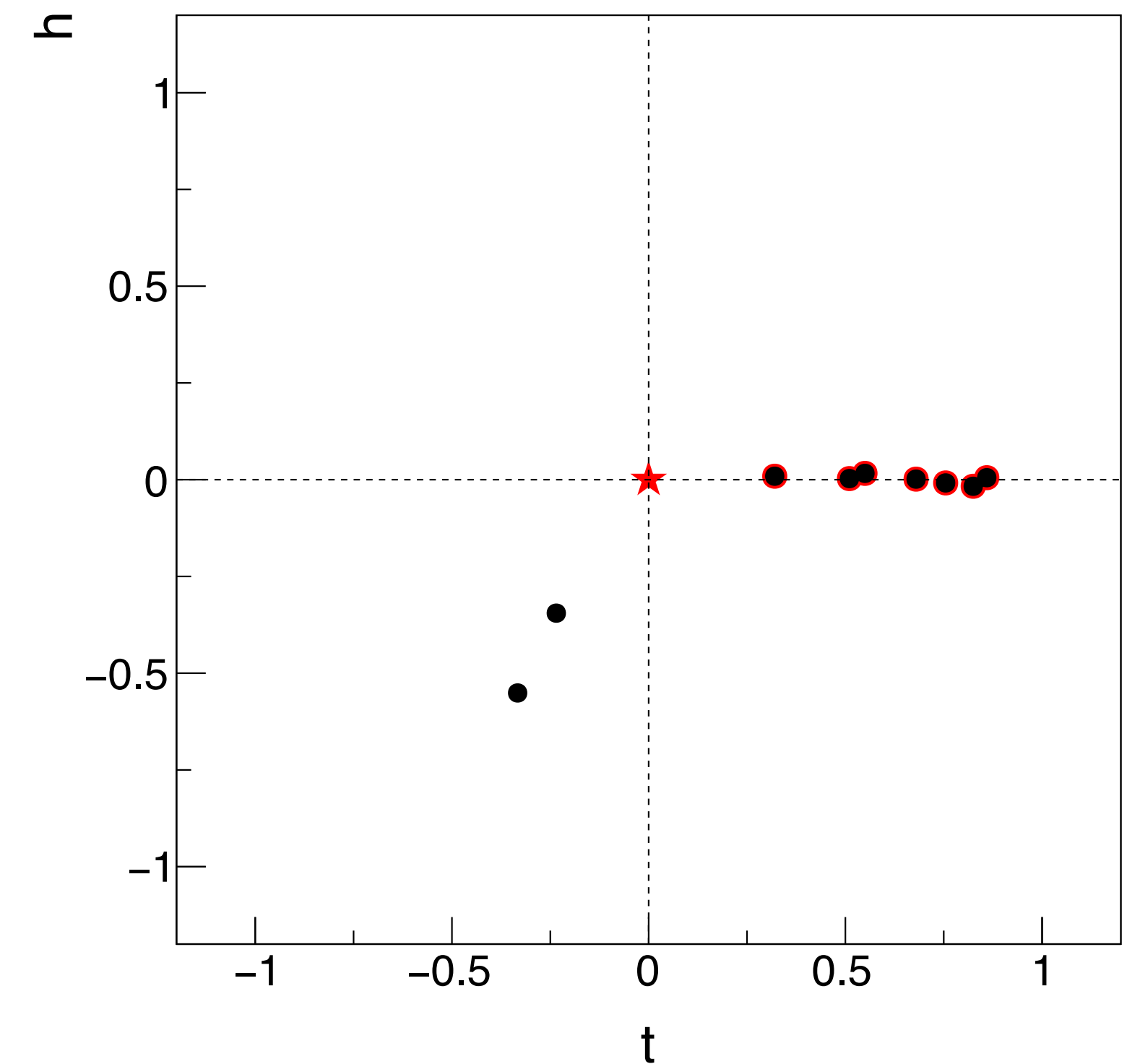
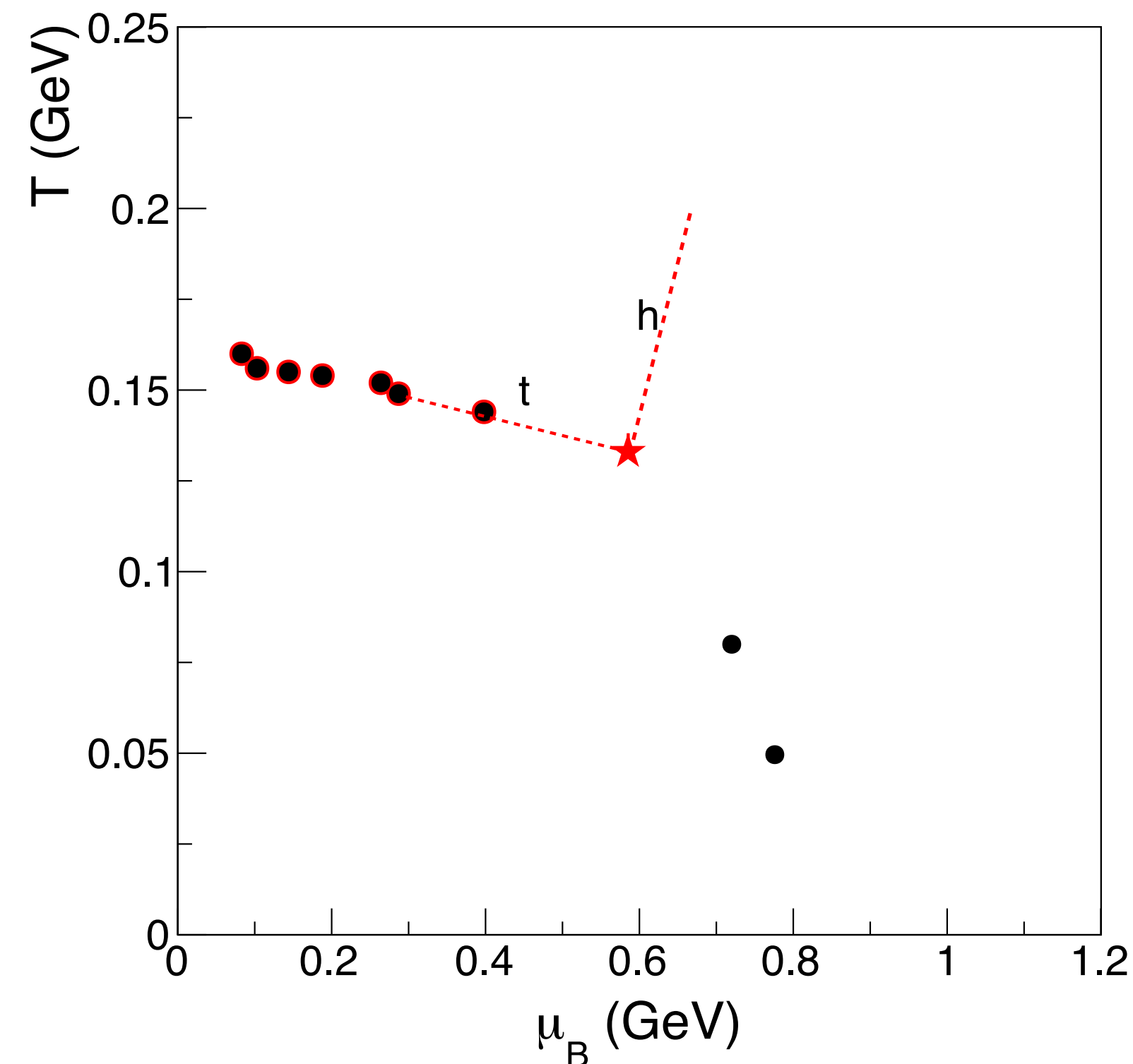
We map ΔT and $\Delta\mu_B$ onto t and h :

- α_1 is determined from a straight line between the candidate CP ($\mu_{B,c}, T_c$) and the $\sqrt{s_{NN}} = 7.7$ GeV freeze-out point
- For the other parameters, we take $\alpha_2 = \alpha_1 + \pi/2$, $w = 1$, and $\rho = \mu_{B,c}/T_c$

$$h(\mu, T) = -\frac{\cos \alpha_1 \Delta T + \sin \alpha_1 \Delta \mu}{w T_c \sin(\alpha_1 - \alpha_2)}$$

$$t(\mu, T) = \frac{\cos \alpha_2 \Delta T + \sin \alpha_2 \Delta \mu}{\rho w T_c \sin(\alpha_1 - \alpha_2)}$$

M.S. Pradeep, M. Stephanov, Phys. Rev. D **100**
5, 056003 (2019) arXiv:1905.13247



Scaled susceptibility: 2D fit w/ mean-field exponents

$$X_L(t_L)L^{-\frac{\sigma}{\nu}} = \phi(tL^{\frac{1}{\nu}})$$

one can find CP by plotting

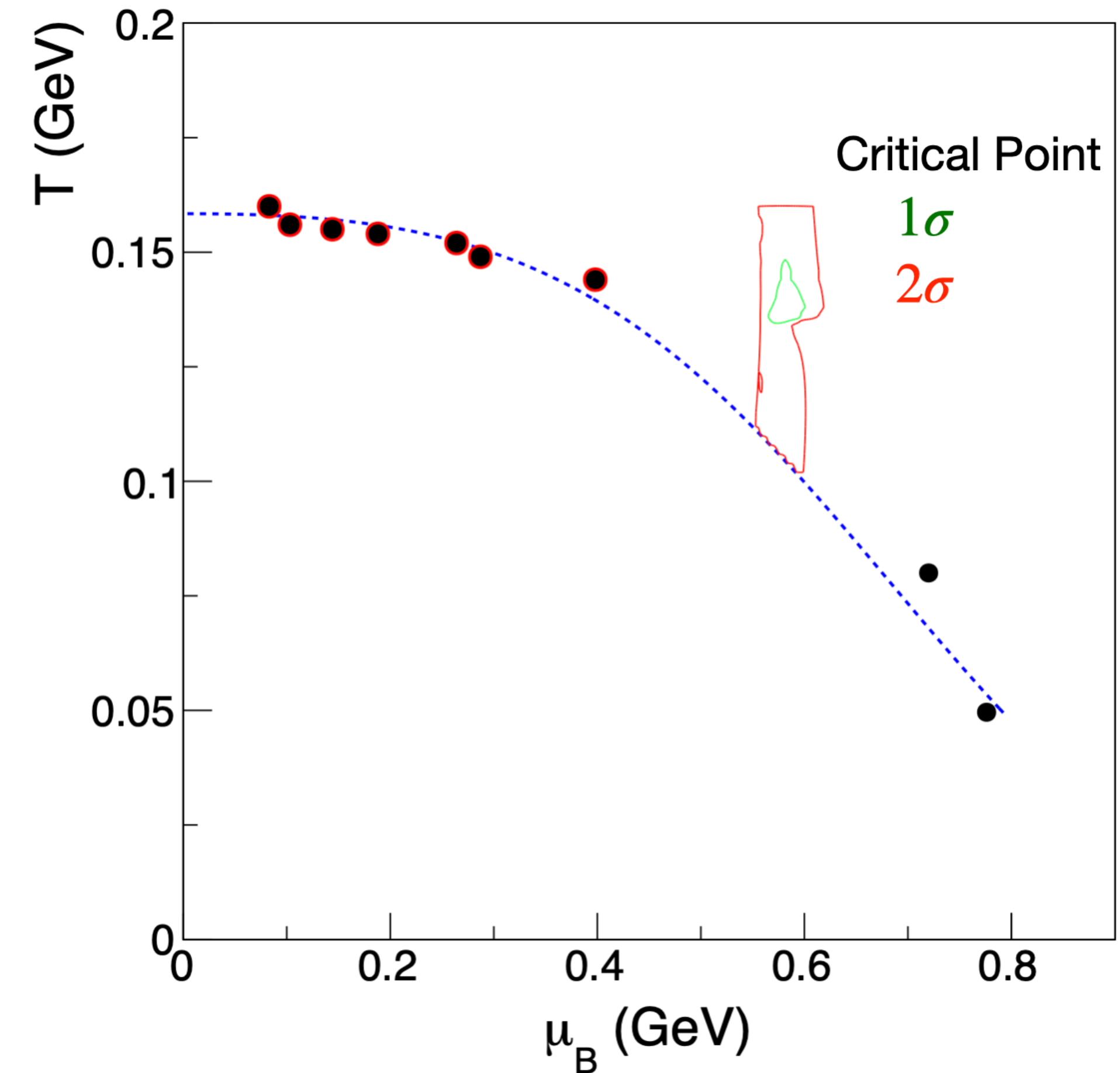
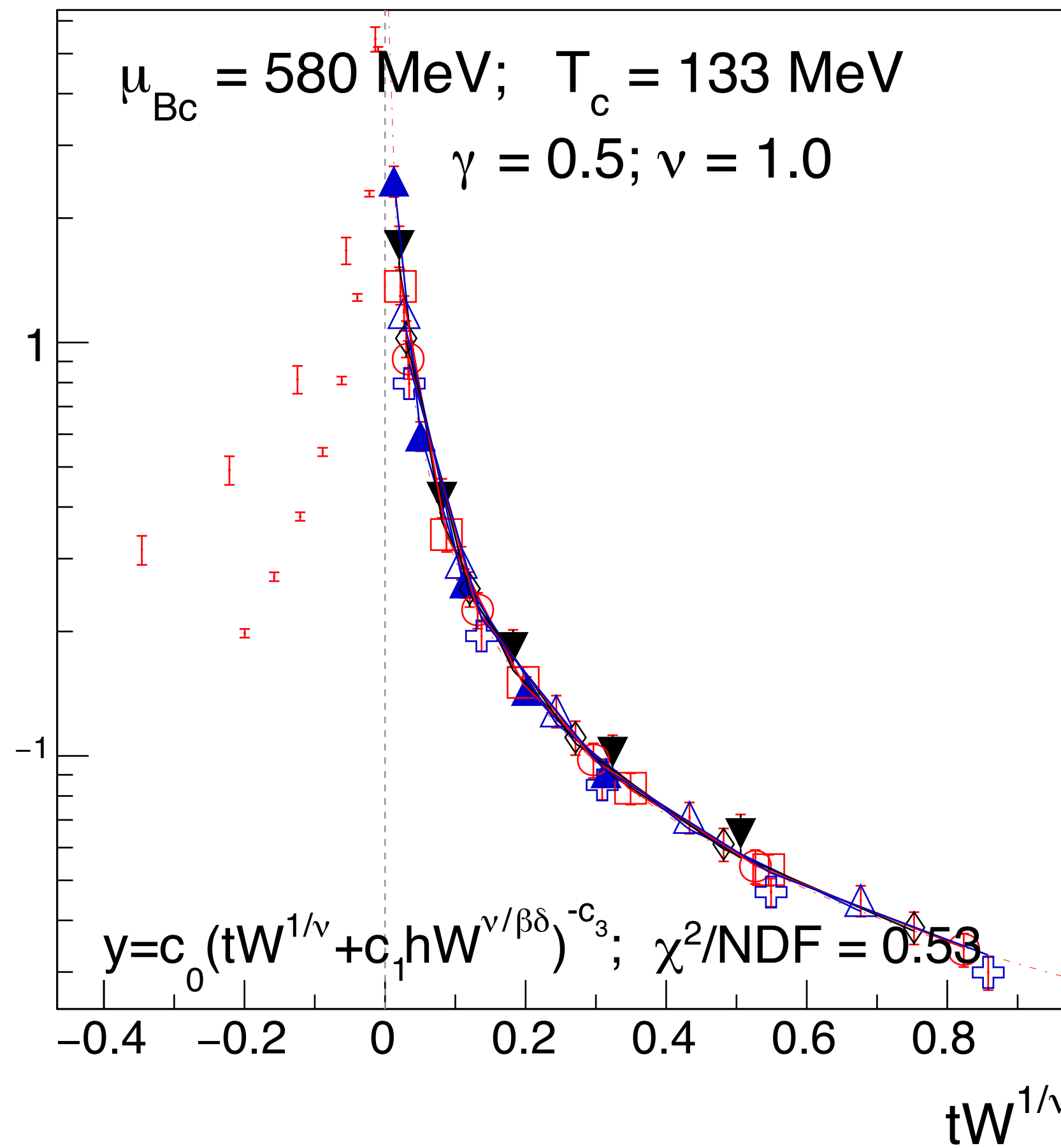
 $\chi_2 W^{-\gamma/\nu}$

$$h(\mu, T) = -\frac{\cos \alpha_1 \Delta T + \sin \alpha_1 \Delta \mu}{w T_c \sin(\alpha_1 - \alpha_2)}$$

$$t(\mu, T) = \frac{\cos \alpha_2 \Delta T + \sin \alpha_2 \Delta \mu}{\rho w T_c \sin(\alpha_1 - \alpha_2)}$$

M.S. Pradeep, M. Stephanov, Phys. Rev. D **100** 5, 056003 (2019) arXiv:1905.13247

$$t \approx -\frac{\mu_B - \mu_{B,c}}{\mu_{B,c}}$$



With mean-field exponents, **we find scaling for $555 < \mu_{B,c} < 610 \text{ MeV}$** ;
 T_c only constrained by “plausibility” (below $T_{pc, \mu_B=0}$ and above T_{fo})

Chi-square contours identify an allowed region in the phase diagram: **$\mu_{B,c} = 580 \pm 30 \text{ MeV}$**

Scaled susceptibility: 2D fit w/ mean-field exponents

$$X_L(t_L)L^{-\frac{\sigma}{\nu}} = \phi(tL^{\frac{1}{\nu}})$$

one can find CP by plotting

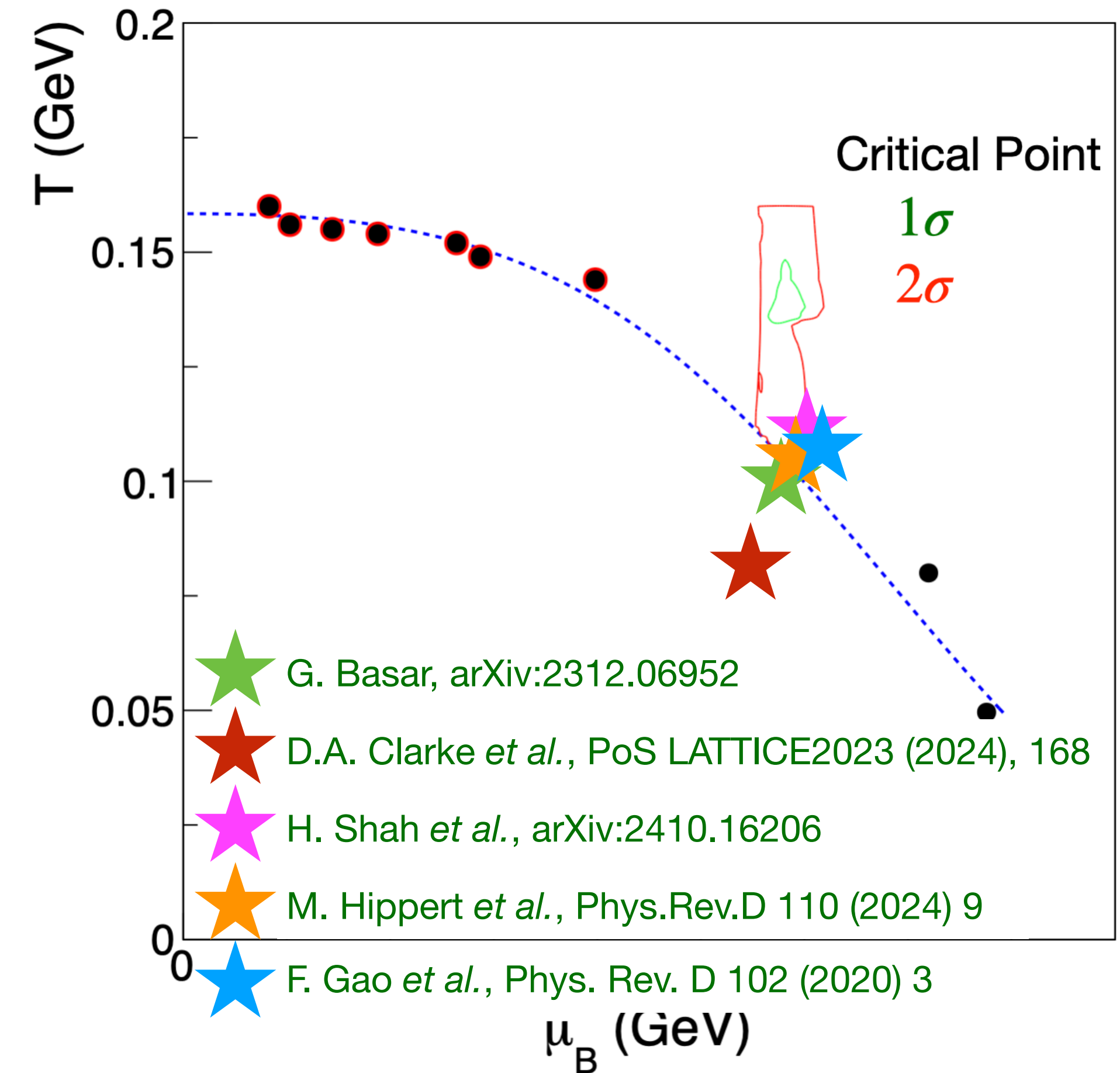
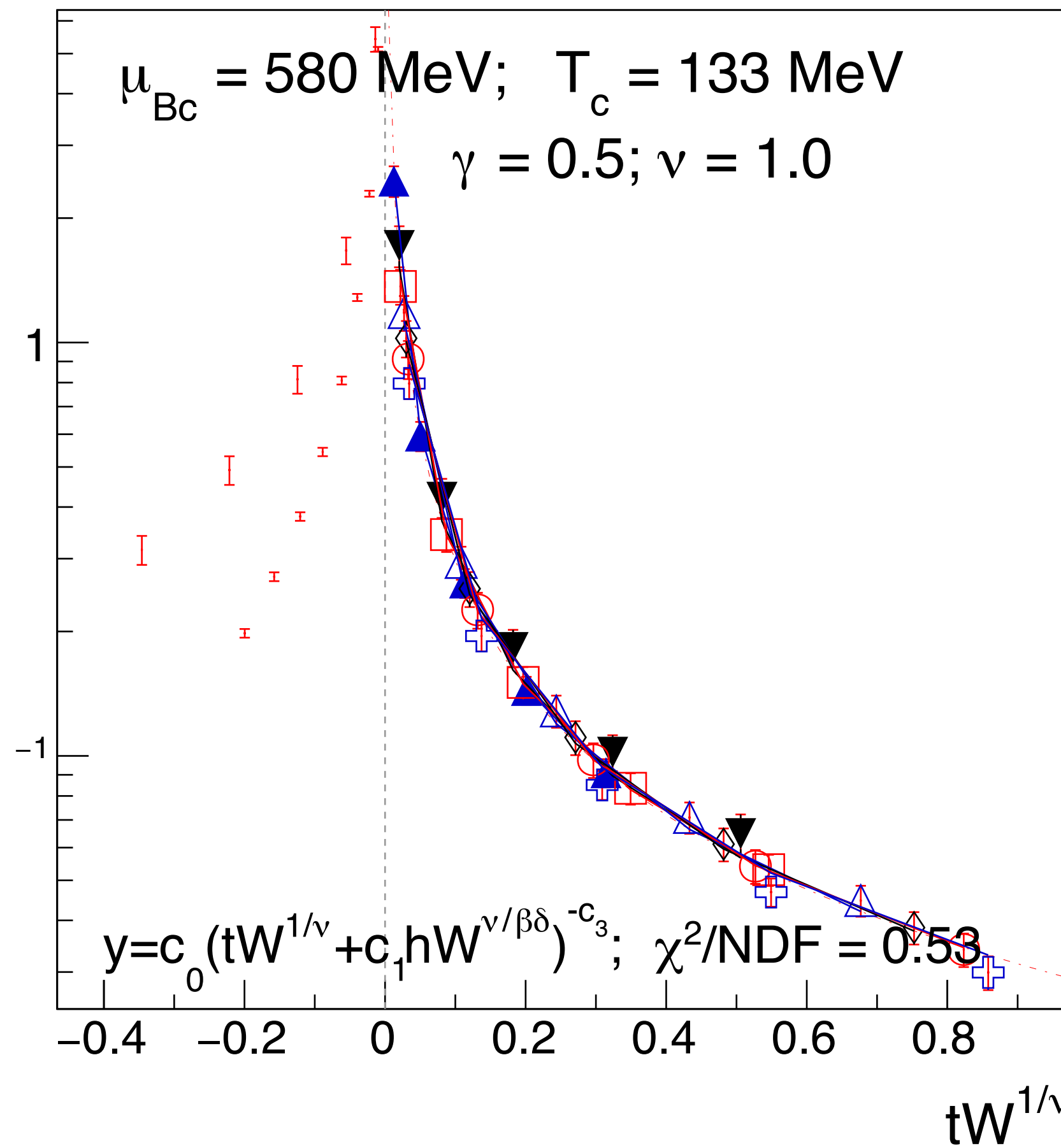
 $\chi_2 W^{-\gamma/\nu}$

$$h(\mu, T) = -\frac{\cos \alpha_1 \Delta T + \sin \alpha_1 \Delta \mu}{w T_c \sin(\alpha_1 - \alpha_2)}$$

$$t(\mu, T) = \frac{\cos \alpha_2 \Delta T + \sin \alpha_2 \Delta \mu}{\rho w T_c \sin(\alpha_1 - \alpha_2)}$$

M.S. Pradeep, M. Stephanov, Phys. Rev. D **100** 5, 056003 (2019) arXiv:1905.13247

$$t \approx -\frac{\mu_B - \mu_{B,c}}{\mu_{B,c}}$$



With mean-field exponents, **we find scaling for $555 < \mu_{B,c} < 610$ MeV;**
 T_c only constrained by “plausibility” (below $T_{pc, \mu_B=0}$ and above T_{fo})

Chi-square contours identify an allowed region in the phase diagram: **$\mu_{B,c} = 580 \pm 30$ MeV**

Scaled susceptibility: 2D fit w/ mean-field exponents

$$X_L(t_L)L^{-\frac{\sigma}{\nu}} = \phi(tL^{\frac{1}{\nu}})$$

one can find CP by plotting

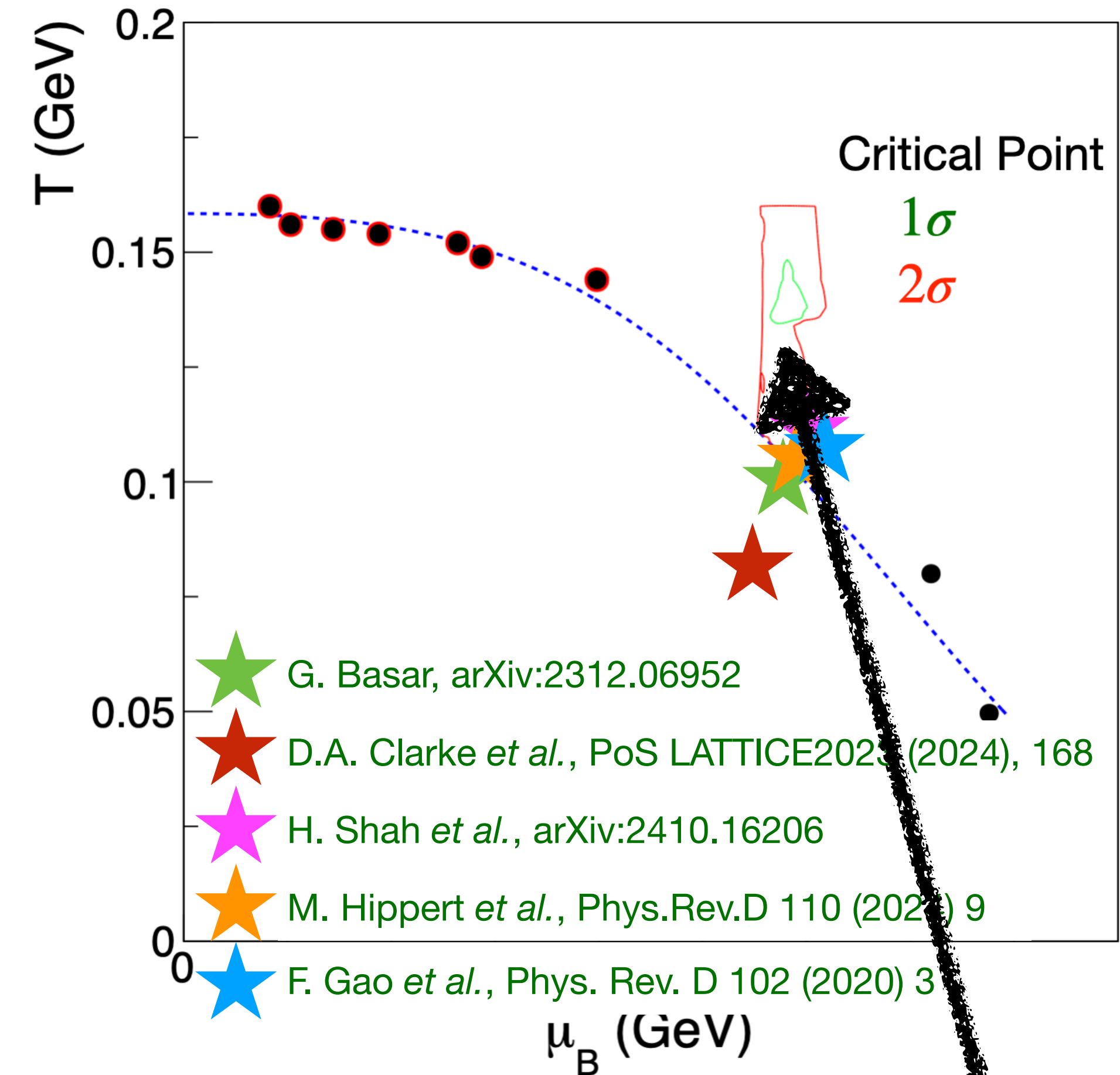
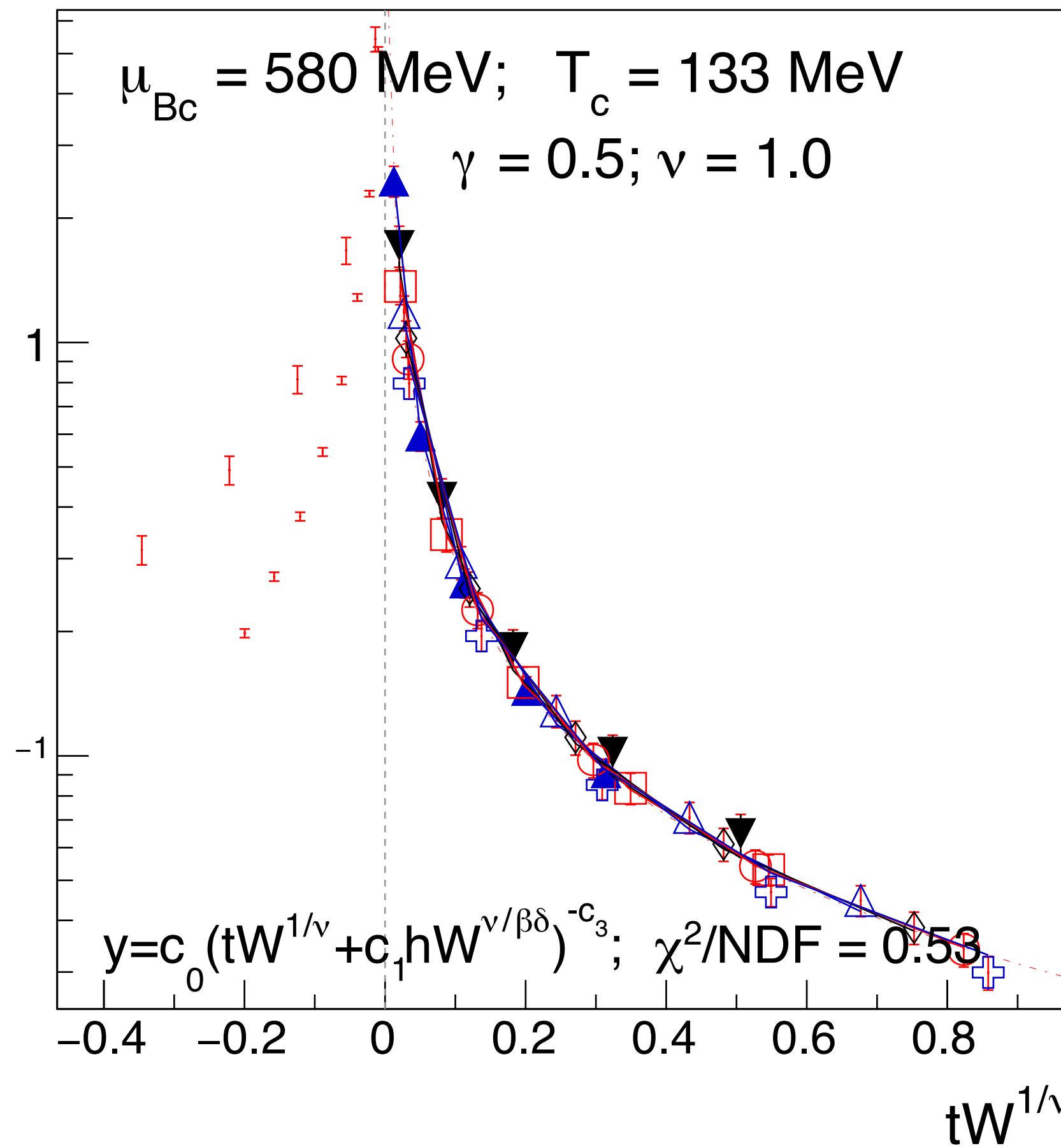
 $\chi_2 W^{-\gamma/\nu}$

$$h(\mu, T) = -\frac{\cos \alpha_1 \Delta T + \sin \alpha_1 \Delta \mu}{w T_c \sin(\alpha_1 - \alpha_2)}$$

$$t(\mu, T) = \frac{\cos \alpha_2 \Delta T + \sin \alpha_2 \Delta \mu}{\rho w T_c \sin(\alpha_1 - \alpha_2)}$$

M.S. Pradeep, M. Stephanov, Phys. Rev. D **100** 5, 056003 (2019) arXiv:1905.13247

$$t \approx -\frac{\mu_B - \mu_{B,c}}{\mu_{B,c}}$$



With mean-field exponents, **we find scaling for $555 < \mu_{B,c} < 610$ MeV**;
 T_c only constrained by “plausibility” (below $T_{pc, \mu_B=0}$ and above T_{fo})

first extraction from experimental data!

Chi-square contours identify an allowed region in the phase diagram: **$\mu_{B,c} = 580 \pm 30$ MeV**

Bonus: Binder cumulant

$$U_4 = -C_4/(3C_2^2) \quad \text{K. Binder, Z. Phys. B 43, 119 (1981)}$$

- Behavior of the Binder cumulant:

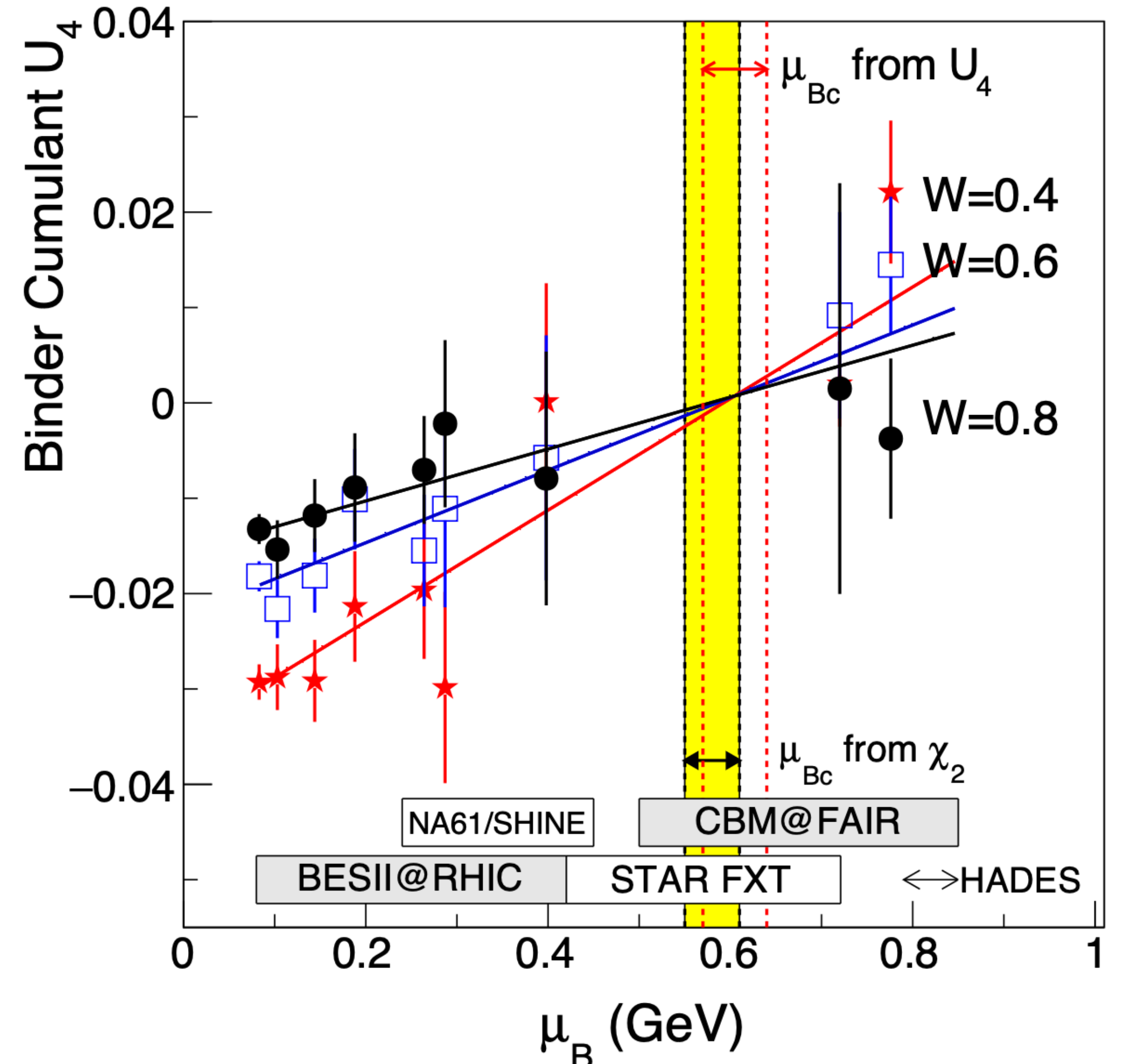
Gaussian: $U_4 = 0$

bimodal: $U_4 = 2/3$

crosses at the critical point:

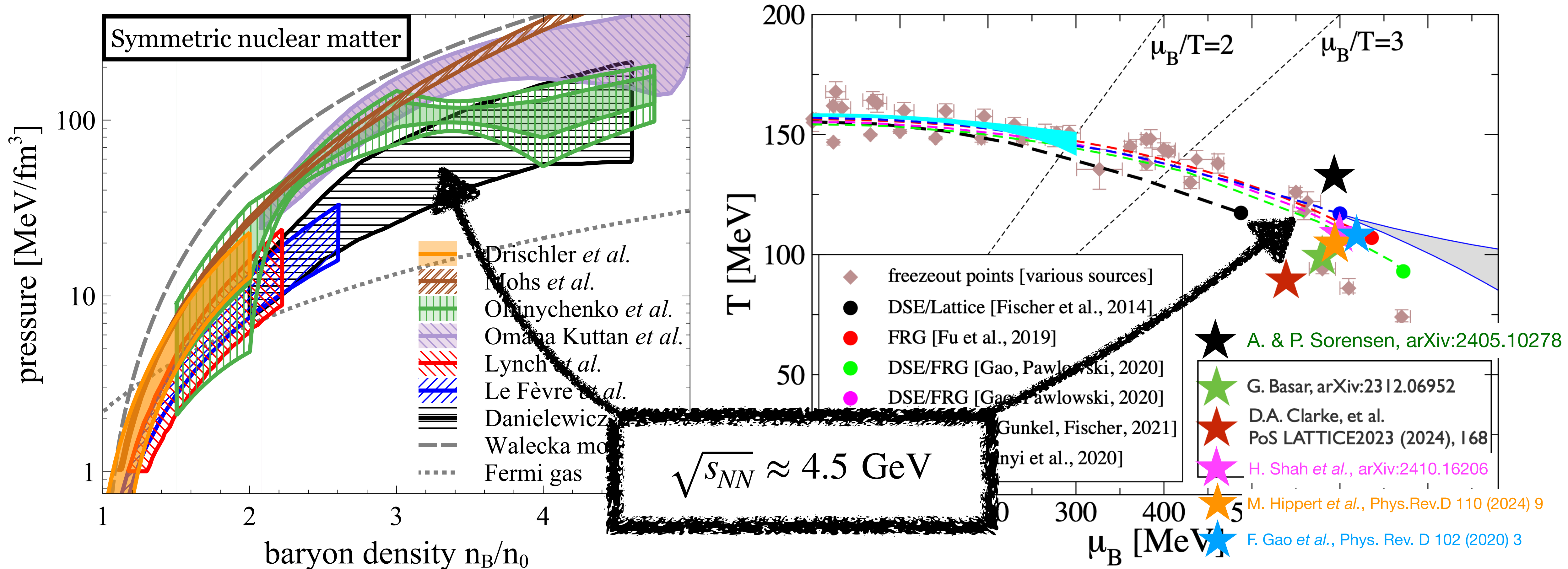
$$U_4 \approx a_1 + a_2(\mu_B - \mu_{B,c})W^{1/\nu}$$

- At low μ_B , U_4 follows Skellam with $U_4(W = 0.8) > U_4(W = 0.6) > U_4(W = 0.4)$
- At $\mu_B > 400$ MeV, the ordering appears to reverse
- Cross at $\mu_B = 605 \pm 35$ MeV, increases toward positive values
- Data are consistent with a critical point between μ_B of 550 and 640 MeV



Summary

- constraints on the n_B -dependence of the EOS: χ EFT, transport model comparisons: old (3) and new (3)
- constraints on the QCD critical point: LQCD-based (3), holography+LQCD (1), STAR data-based (1)



adapted from Christian Fischer, CPOD 2024